



Assessing heat vulnerability risk of Jinan and Guangzhou's older populations based on multisource remote sensing data

Jifei Chen ^a, Xiaoming Shi ^a, Yongying Shi ^b, Laurence L. Delina ^{a,*}

^a Division of Environment and Sustainability, The Hong Kong University of Science and Technology, Clear Water Bay, Kowloon, Hong Kong Special Administrative Region of China

^b The First Affiliated Hospital of Guangzhou Medical University, Guangzhou, Guangdong, China

ARTICLE INFO

Keywords:

Climate change
Heat vulnerability
Older adults
Geodetector
China

ABSTRACT

As climate change intensifies, understanding heat vulnerability – defined as the susceptibility of populations to the adverse effects of heat waves – becomes increasingly critical for effective adaptation and management strategies. This study uses an “Exposure-Sensitivity-Adaptation” framework combined with GeoDetector to assess heat vulnerability in Jinan and Guangzhou. The analysis incorporates Land Surface Temperature (LST), Normalized Difference Vegetation Index (NDVI), population density, Points of Interest (POI), and socioeconomic data. These factors are used to construct a comprehensive index system and a vulnerability measurement model focused on assessing the heat vulnerability of older populations. This study identifies vulnerable spatial regions and reveals the key factors driving heat vulnerability, offering valuable insights into its spatial dynamics and underlying causes in urban areas. The results show significant spatial disparities in heat vulnerability between and within the two cities. In Guangzhou, the core urban districts, such as Tianhe and Yuexiu, exhibit lower vulnerability due to robust infrastructure, higher disposable incomes, and extensive green space coverage. In contrast, peripheral districts, including Conghua and Zengcheng, face higher vulnerability due to uneven resource distribution and slower urbanisation. In Jinan, the urban core, including Shizhong and Licheng districts, demonstrates lower vulnerability supported by modern infrastructure and medical resources, while peripheral areas, such as Shanghe County and parts of Zhangqiu, show heightened vulnerability driven by ageing populations, limited healthcare, and lower economic development. At the community level, high-risk areas are clustered in economically disadvantaged neighbourhoods and regions with dense older populations. In Guangzhou, high-vulnerability communities (e.g., Beijing, Binjiang, and Datang) are in peripheral districts or underdeveloped areas with limited resources. Similarly, in Jinan, high-risk communities (e.g., Guanzhaying, Hongjialou, and Huanghe) are concentrated in peripheral counties and older urban neighbourhoods with ageing populations. To mitigate heat vulnerability, the study recommends enhancing urban green spaces, retrofitting ageing infrastructure, and implementing community-specific education campaigns. These findings provide actionable insights into tailoring urban planning and climate adaptation strategies to improve heat resilience, particularly in rapidly urbanising cities with ageing populations and socio-economic inequalities.

1. Introduction

The rise in global temperatures has significantly increased the frequency, intensity, and duration of extreme heat events, posing severe risks to ecosystems, human health, and socio-economic stability [1]. By 2100, global megacities are expected to experience more frequent and intense heatwaves, with low-income and rapidly urbanising cities in southern Asia, such as those in India and Southeast Asia, disproportionately affected [2]. Similar trends are projected for urban regions

worldwide. Studies estimate that by 2050, over 350 million people in cities across the globe will be exposed to deadly heat conditions for at least 20 days per year, even if greenhouse gas emissions are dramatically curbed [3]. Regions as diverse as North America, Europe, the Middle East, and Australia all face substantially increased threats of heatwaves under various climate scenarios [4,5]. In Africa, climate projections indicate that heatwaves, which are currently rare, could become regular occurrences by 2040 in half of the region's areas due to ongoing climate changes [6]. In Japan and South Korea, cities like Tokyo and Seoul have

* Corresponding author.

E-mail address: lld@ust.hk (L.L. Delina).

<https://doi.org/10.1016/j.buildenv.2025.112622>

Received 18 November 2024; Received in revised form 14 January 2025; Accepted 24 January 2025

Available online 29 January 2025

0360-1323/© 2025 Elsevier Ltd. All rights are reserved, including those for text and data mining, AI training, and similar technologies.

already seen increased heat-related mortality, which could become more severe as temperatures rise [7]. In China, projections suggest that by the end of the 21st century, up to 1.18 billion people could be affected by heat waves, underscoring the urgent need for robust heat risk management strategies [8].

The health risks associated with extreme heat are particularly severe. Several studies have linked heat waves to higher morbidity and mortality rates from heat-related conditions, such as cardiovascular diseases and respiratory issues [9–11]. Evidence of increased morbidity and mortality during heat waves in China emphasises the need for a robust risk assessment framework to inform early warning systems and public health interventions [12].

In addition, China is facing a demographic transition, with its population aged 65 and older projected to more than double from 172 million (12 % of the population) in 2020 to 366 million (26 %) by 2050 [13]. This rapidly ageing population is particularly vulnerable to the impacts of climate change, especially extreme heat. Older adults face heightened heat-related health risks due to physiological changes associated with ageing, such as decreased sweat gland output, reduced skin blood flow, and impaired thermoregulation, which weaken the body's ability to cope with high temperatures [14]. Pre-existing health conditions common among older populations, such as cardiovascular diseases and diabetes, further exacerbate their vulnerability, increasing the risk of heat-related morbidity and mortality [15]. Older adults living alone or with limited social networks often struggle to access cooling resources or receive timely assistance during heat waves, amplifying their risk of adverse outcomes [16]. Despite these well-documented vulnerabilities, few studies have explicitly examined how extreme heat affects older adults locally, particularly in rapidly ageing urban contexts like those in many Chinese cities [17]. This lack of attention is concerning given the unique challenges of urbanisation, social isolation, and disparities in access to adaptive resources.

Early research primarily focused on physical exposure to extreme heat using quantitative, data-driven approaches. For instance, El-Zein et al. [18] utilised a multi-criteria outranking approach to assess climate change vulnerability, explicitly focusing on heat stress in Sydney. Hu et al. [19] employed daily maximum and minimum temperature data from meteorological stations to estimate hazards during extreme heat events (EHes). Stéphanne et al. [20] integrated Earth Observation data with geospatial analyses to assess exposure in urban areas, emphasising the importance of combining diverse data sources. Kwon et al. [21] explored sensible heat flux to assess thermal vulnerability in Seoul, Korea, finding that identifying thermally vulnerable areas based on sensible heat flux was more objective and spatially accurate than using traditional temperature-based approaches. While these studies provided valuable insights into exposure, they often neglected broader socio-environmental factors.

Subsequent studies began incorporating more comprehensive frameworks, recognising the importance of social vulnerability and adaptive capacity. For example, Shih et al. [22] provided insights into heat vulnerability in subtropical regions through expert judgments, underscoring the complexities of incorporating socio-environmental factors into assessments. Puntub et al. [23] applied future-oriented vulnerability scenarios to address human heat stress in Bonn, Germany, highlighting the importance of integrating climate trajectories and urban development scenarios. Similarly, Wu et al. [24] used remote sensing to map heat-health vulnerability in Karachi, redefining heat-wave mortality risks and categorising vulnerability into different levels. These studies marked a shift toward multi-dimensional approaches but often lacked localised, community-specific analysis.

Despite these advancements, many earlier approaches were limited by their focus on isolated factors, such as temperature thresholds or demographic profiles, without fully considering the intersection of environmental, social, and infrastructural dimensions. Unlike earlier approaches, the ESA framework integrates environmental hazards, social vulnerability, and adaptive capacity to provide a nuanced

understanding of vulnerability. Dong et al. [25] applied the ESA framework to map urban heat risks in megacities, demonstrating its ability to capture the interplay between heat stress, socio-economic inequalities, and infrastructural limitations. Similarly, Lo et al. [26] and Dubey et al. [27] employed the ESA framework to assess the spatial variability of heatwave risks, emphasising the importance of adaptive capacity in mitigating vulnerability. However, despite these studies using the ESA framework, they still fail to address localised and community-specific vulnerabilities, particularly in regions with distinct climatic and socio-economic characteristics.

This study builds on the ESA framework by incorporating remote sensing data, demographic indicators, and adaptation resources to assess the heat vulnerability of older populations in Jinan and Guangzhou, two Chinese cities with unique climatic and socio-economic contexts. While previous research has predominantly adopted macro-level assessments, often overlooking localised nuances, this study focuses on community-scale impacts with an emphasis on vulnerable older populations. By concentrating on community-scale impacts and integrating adaptation resources (e.g., metro access, healthcare facilities, and green spaces), this study offers a novel approach to evaluating heat vulnerability. This localised approach reveals how extreme heat uniquely affects vulnerable populations and provides insights with broader implications for urban planning and climate resilience in rapidly ageing and urbanising regions across Asia and globally.

This study has two main objectives: (1) to investigate the spatial distribution of high-temperature vulnerability in Jinan and Guangzhou and (2) to explore the driving factors contributing to heat vulnerability. Section 2 provides an overview of the study areas, and the data utilised. Section 3 outlines the methodology. Section 4 presents the results, and Section 5 discusses the main findings. Section 6 highlights the study's limitations and identifies potential research directions.

2. Study cities and data

2.1. Study cities

Jinan and Guangzhou, with 161 and 170 communities, respectively, were selected as representative case studies of northern and southern Chinese cities (Fig. 1). Their climate, urban structure, and socioeconomic development differences offer valuable insights for comparing how geographical context influences heat vulnerability distributions [12]. This comparative approach uncovers fundamental principles of urban heat vulnerability and provides a scientific basis for tailored adaptation strategies at the local level.

The city of Jinan, located in central-western Shandong (36°40'N, 117°00'E), is an economic, political, and cultural hub. As of April 2024, Jinan comprises ten districts and two counties, covering 10,244 km² [28]. Jinan experiences a temperate continental climate, with an annual average temperature, precipitation, and sunshine of 15.4 °C, 638.3 mm, and 6.85 h per day, respectively [29]. In 2023, Jinan's GDP reached CNY1.28 trillion (USD 1795.84 billion) with a population of 9.44 million, of which 7.1 million (75.3 %) resided in urban areas [30]. Despite its economic success, Jinan faces challenges such as intense heat waves, earning it the title of China's "Four ovens" [31]. The impact of global warming is evident in Jinan, as the city experienced 35 "extremely hot" days (defined as days with the daily maximum temperature reaching or exceeding 35 °C) in 2023, setting new records [29].

Guangzhou is the capital of Guangdong Province and is in the Pearl River Delta (23°13'N, 113°27'E). In 2023, Guangzhou covered an area of 7434 km² and was home to 18.83 million residents, boasting a GDP that exceeded CNY 3 trillion (USD 4212 billion). The average urban disposable income in 2023 was CNY 44,771 (USD 3187.70), showing a 4 % annual increase [32]. Guangzhou experiences a subtropical monsoon climate, with an annual mean temperature of 22 °C and precipitation exceeding 1800 mm over approximately 150 rainy days [33]. However, 2023 saw unprecedented extreme heat, shattering records with a

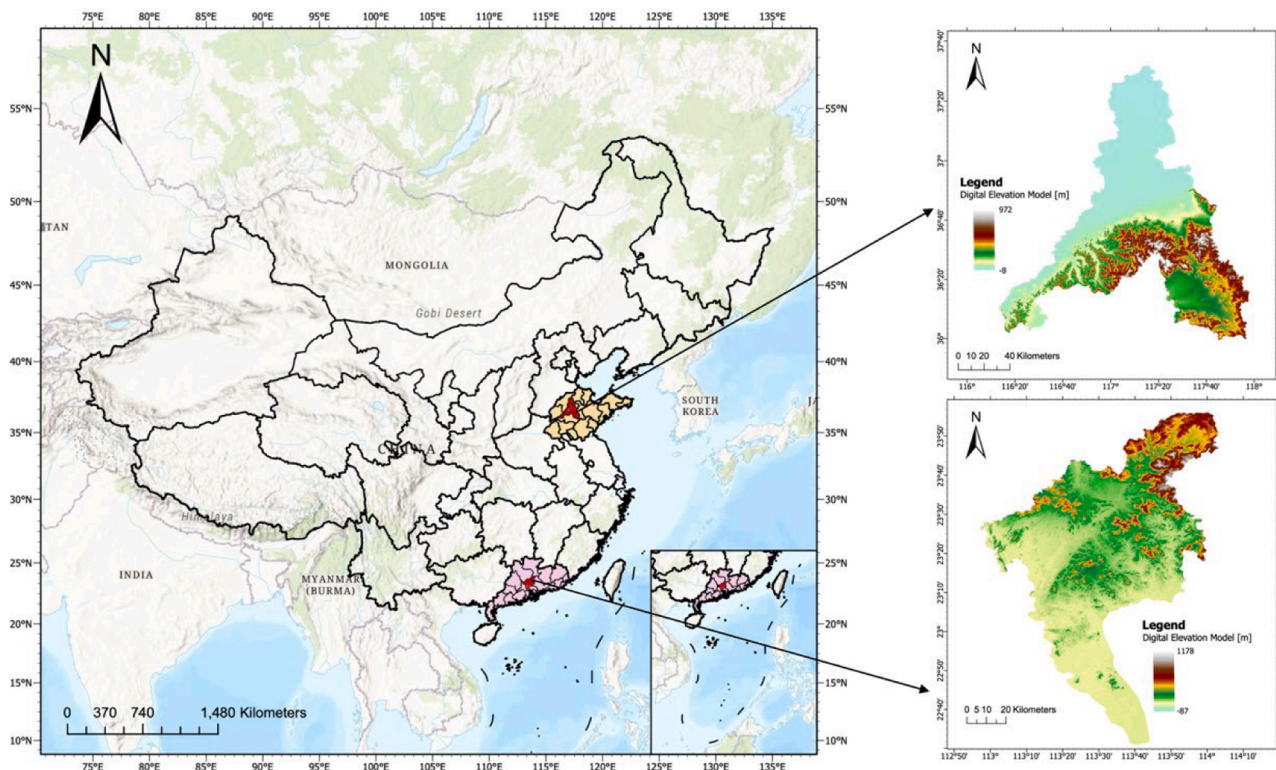


Fig. 1. Study areas.

maximum temperature of 36.4 °C [33].

2.2. Data sources

- (1) Land surface temperature (LST) data from the TRIMS LST-TP daily 1-km all-weather LST dataset provided by the National Tibetan Plateau Data Center (TPDC, <https://data.tpdc.ac.cn/en/data/05d6e569-6d4b-43c0-96aa-5584484259f0/>), used to assess heat exposure [34]. This dataset covers mainland China and surrounding areas from 2000 to 2022 and has a temporal resolution of 4 observations per day and a spatial resolution of 1 km.
- (2) Landsat Normalized Difference Vegetation Index (NDVI) data derived from Google Earth Engine processing of Landsat satellite imagery from the National Ecosystem Science Data Center [35], used to represent vegetation cover. It has a spatial resolution of 30 m and a temporal resolution of annual maximum NDVI values.
- (3) Population data, including total population density, older population ratio, older population density, and highly educated population from the Seventh National Population Census Communique [36], used for heat sensitivity assessment.
- (4) Facility data of hospital numbers, metro stations, shopping malls, and gardens from OpenStreetMap represent urban adaptability [37]. Per capita disposable income data from the Jinan Statistical Yearbook [30] and Guangzhou Statistical Yearbook [38] measure economic adaptability. POI and PCDI data are used for heat adaptation assessment.

The MODIS LST and NDVI files from July to September in China were imported into ArcGIS Pro 2022 to create average temperature and vegetation index rasters. The summer solstice period was chosen to capture peak summertime heat exposure by calculating the mean LST and NDVI, which account for variability across the summer months. Spatial and temporal aggregation was performed using the Cell Statistics tool in ArcGIS Pro. Additionally, raw population and POI data

underwent quality control, including outlier removal, coordinate system standardisation to WGS 1984, clipping to the study area, and projection to an appropriate analysis coordinate reference system. Population, PCDI, and POI datasets were aggregated and summarised by community boundaries to align with the 331 spatial analysis units. Finally, using the preprocessed LST, NDVI, population, and POI data layers, a vulnerability assessment index system was constructed with indicators assigned to each community polygon.

Table 1 summarises the data sources used to assess heat exposure, sensitivity, and adaptation in our study.

3. Methodology

This study employs the “Exposure-Sensitivity-Adaptation” framework outlined in the Intergovernmental Panel on Climate Change (IPCC) Sixth Assessment Report [39] (refer to Fig. 2). The heat vulnerability index is calculated using a composite index approach and is visually represented through overlay mapping to illustrate variations across different areas. As climate change intensifies, urban heat challenges are increasingly significant, posing severe threats to human health and socioeconomic development. Hence, a thorough understanding of the spatial distribution of heat vulnerability and its influencing factors is crucial for devising effective adaptation strategies and enhancing urban climate resilience. The entropy weight method determines the weights of various factors within the dimensions of exposure, sensitivity, and adaptability.

3.1. Data standardisation

To ensure consistency among different indicators and improve the accuracy of the results, the data for all indicators were standardised. Each indicator was categorised as positive or negative based on its relationship with vulnerability. In this study, the min-max normalisation method was applied to standardise all indicators within the range of 0 to 1, as expressed in (Eq. (1)):

Table 1
Data sources for heat exposure, sensitivity, and adaptation assessment.

Vulnerability aspect	Variable	ID	Expected impact on Heat Risk Index	Sources
Exposure	Land Surface Temperature (LST)	E-01	Positive	Zhou et al. [34]
	The Normalized Difference Vegetation Index (NDVI)	E-02	Negative	Dong et al. [35]
Sensitivity	Total population density	S-01	Positive	National Bureau of Statistics of China [36]
	Older population density	S-02	Positive	
	Older population proportion	S-03	Positive	
Adaptation	Garden	A-01	Positive	OpenStreetMap [37]
	Per capita disposable income	A-02	Positive	Jinan Municipal Bureau of Statistics [30] Guangzhou Municipal Bureau of Statistics [38]
	Hospital	A-03	Positive	OpenStreetMap [37]
	Shopping mall	A-04	Positive	
	Metro station	A-05	Positive	
	High-level education	A-06	Positive	National Bureau of Statistics of China [36]

Positive indicators:

$$N_{ij} = \frac{x_{ij} - \min(x_{ij})}{\max(x_{ij}) - \min(x_{ij})} \quad (1)$$

Negative indicators:

$$N_{ij} = \frac{\min(x_{ij}) - x_{ij}}{\max(x_{ij}) - \min(x_{ij})} \quad (2)$$

Where, N_{ij} is the dimensionless number after standardisation; x_{ij} is the original data value of each indicator; $\max(x_{ij})$ and $\min(x_{ij})$ are the maximum and minimum values of the j -th indicator respectively. These values are used in the min-max normalisation process to rescale the original data from 0 to 1.

3.2. Determination of the weight of evaluation indicators

The weights indicate how much each indicator in the criterion layer influences the target layer. Each indicator must be weighed to assess heat vulnerability levels based on different factors. This study used the hierarchical analysis method (AHP) and the entropy weight method (EWM) to calculate the subjective and objective weights of 11 heat vulnerability indicators, which helps overcome the limitations of using either purely subjective or objective methods alone [40].

3.2.1. AHP method to determine subjective weights of indexes

The Analytic Hierarchy Process (AHP) incorporated experts' subjective input to score the indicators' importance [41]. This method involves a systematic process with four main steps: first, the hierarchical structure of indicators is established based on the relationships between them; second, a judgment matrix is constructed, where each element represents the relative importance of one indicator compared to another; third, the consistency of the judgment matrix is assessed to ensure the rationality of the evaluations; and finally, the weights of the indicators are calculated through normalisation [42]. The formula is expressed as:

$$A = (a_{ij})_{n \times n} \quad (3)$$

Where a_{ij} represents the j -th indicator.

$$P_i = \left(\prod_{j=1}^n a_{ij} \right)^{\frac{1}{n}} \quad (4)$$

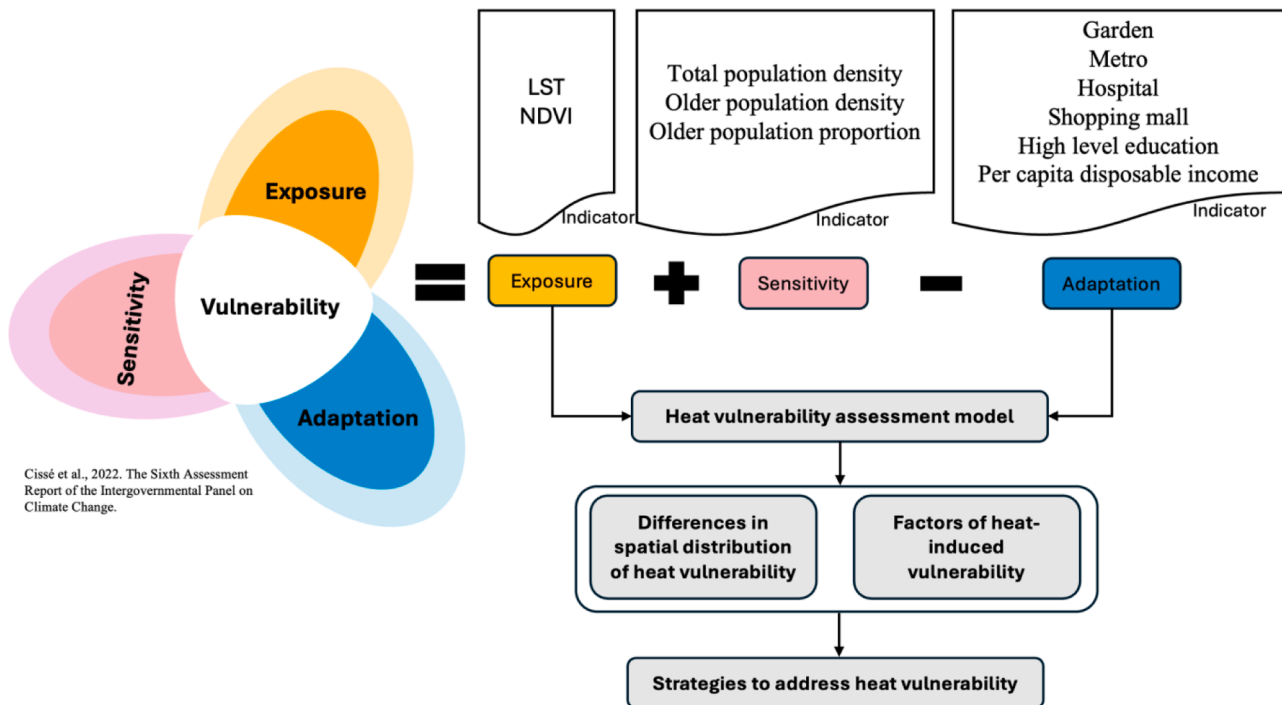


Fig. 2. Heat vulnerability assessment framework.

$$\tau_i = \frac{P_i}{\sum_i^n P_i} \quad (5)$$

Where p_i is the priority vector calculated from the geometric mean, and τ_i represents the final subjective weight of the i th indicator.

3.2.2. Entropy weight method

Compared to AHP, the EWM effectively avoids the subjectivity of artificially determining the weight of indicators [43]. The entropy weight method determines the weight based on the difference in information between the data. If the information entropy of the indicator is smaller, it indicates a higher degree of disorder and a larger range of change, thus exerting a more significant impact on the evaluation. Excel was used to determine the weights for the indicators in Table 2. The final scores for each indicator in each community can be found in Section 4 and Appendix A.

The calculation steps of the entropy weight method involve (Eq. (6)) calculating information entropy:

$$H_j = -k \sum_{i=1}^m p_{ij} \ln p_{ij} \quad (6)$$

Where H_j represents the information entropy value of the i th indicator.

$$p_{ij} = z_{ij} / \sum_{i=1}^m z_{ij}, \quad k = 1 / \ln m \quad (7)$$

Where P_{ij} is the proportion of the indicator in the sample and (Eq. (8)) calculating the indicator weight:

$$w_j = \frac{1 - H_j}{\sum_{i=1}^n (1 - H_j)} \quad \text{and } w_j \in [0, 1], \quad \text{and } \sum_{j=1}^n w_j = 1 \quad (8)$$

3.2.3. Combination weighting method

The objective entropy weights and subjective AHP weights were integrated through the following formulas to generate the comprehensive indicator weights:

$$\lambda = (\tau + w) / 2 \quad (9)$$

3.3. Heat exposure assessment

The assessment of exposure is mainly based on two factors: LST and NDVI. LST directly indicates the thermal conditions of urban surfaces and is crucial for assessing the urban heat island effect [44]. NDVI measures the amount of urban greenery, which can effectively reduce

Table 2
Weights of heat exposures, sensitivities, and adaptation indicators in Jinan and Guangzhou.

Factors	Indicators	Comprehensive weight (Jinan)	Comprehensive weight (Guangzhou)
Exposure	LST	0.520	0.516
	NDVI	0.480	0.484
Sensitivity	Total population density	0.303	0.241
	Old population density	0.472	0.502
	Old population proportion	0.225	0.257
Adaptation	Shopping mall	0.104	0.119
	Garden	0.298	0.339
	Metro	0.251	0.141
	Hospital	0.101	0.141
	High education level	0.097	0.109
	PCDI	0.149	0.151

ambient temperatures by evapotranspiration, thus helping to mitigate the heat island effect [45]. The combined considerations of LST and NDVI comprehensively characterise urban thermal environments and their potential for cooling. The entropy weight method combines these indicators into an integrated exposure index. The exposure index is then divided into five risk levels using the natural classification method (Jenks Natural Breaks method), a commonly used algorithm in GIS applications [46]. This method effectively partitions a dataset into a pre-defined number of homogeneous categories by minimising variance within groups and maximising variance between groups [47]. Based on the heat vulnerability indicator weight (Table 2), the heat exposure for each indicator factor is calculated using (Eq. (10)):

$$HEA = \sum_{i=1}^n (w_{ei} \times h_{ei}) \quad (10)$$

Where HEA is the heat exposure index; w_{ei} is the weight of the i th indicator of heat exposure; h_{ei} is the standardised value of a single indicator, and n represents the number of indicators.

3.4. Heat sensitivity assessment

The sensitivity assessment focuses on inherent population characteristics, especially the proportion of older residents. Older individuals are particularly concerned due to their diminished physiological regulation and reduced heat tolerance, which render them more vulnerable during heat waves [48]. Research indicates a notably higher mortality rate among older individuals during heat waves [49]. Heat sensitivity indicators include total population density, proportion of the population aged 60 years and above, and population density. The higher the heat sensitivity, the higher the heat vulnerability. Based on the heat vulnerability indicator weight (Table 2), the heat sensitivity for each indicator factor is calculated using (Eq. (11)):

$$HSA = \sum_{i=1}^n (w_{ei} \times h_{ei}) \quad (11)$$

Where HSA is the heat sensitivity index; w_{ei} is the weight of the i th indicator of heat sensitivity; h_{ei} is the standardised value of a single indicator, and n represents the number of indicators.

3.5. Heat adaptability assessment

Urban structures that aid in mitigating and safeguarding against heat waves are considered when evaluating adaptability. Key indicators include the presence and number of gardens, hospitals, metro stations, and socioeconomic factors such as education level and income. Urban parks serve as cooling and refuge areas, providing essential green spaces [50]. The quantity of hospitals signifies the availability of healthcare services during heat waves [51]. Metro stations and shopping malls serve as vital cooling shelters, especially for lower-income residents without air conditioning [52]. The education level reflects residents' awareness and access to heatwave information, contributing to better preparedness [53]. PCDI represents the capacity to procure and use cooling devices like air conditioners [54]. The stronger the adaptability to heat, the lower the heat vulnerability. Based on the heat adaptability indicator weight (Table 2), the heat adaptability for each indicator factor is calculated using (Eq. (12)):

$$HAA = \sum_{i=1}^n (w_{ei} \times h_{ei}) \quad (12)$$

Where HAA is the heat adaptability index; w_{ei} is the weight of the i th indicator of heat adaptability; h_{ei} is the standardised value of a single indicator, and n represents the number of indicators.

3.6. Heat vulnerability assessment

This study adapts the Climate Change Vulnerability Index (CCVI) model modified to construct a heat vulnerability assessment framework. The framework includes an equation that quantifies heat vulnerability, using exposure and sensitivity as positive indicators and adaptive capacity as a negative indicator [55].

Fig. 2 illustrates a framework for assessing heat vulnerability based on exposure, sensitivity, and adaptation. This model combines key indicators to evaluate heat vulnerability within urban populations, developed by Cissé et al. [39] in the Sixth Assessment Report of the Intergovernmental Panel on Climate Change. This model combines key indicators to evaluate heat vulnerability within urban populations. **Exposure** is represented by environmental factors, specifically Land Surface Temperature (LST) and Normalized Difference Vegetation Index (NDVI). These indicators measure the extent to which a population is exposed to heat, where higher LST and lower NDVI values typically indicate greater heat exposure. **Sensitivity** captures the demographic factors influencing vulnerability, such as total population density, older population density, and older population proportion. These factors affect how intensely a population might feel the impact of heat, with denser and older populations being more sensitive. **Adaptation** encompasses social and infrastructural factors that may mitigate heat effects, including proximity to gardens, metro access, hospitals, shopping malls, and indicators of socioeconomic resilience, like high education levels and per capita disposable income. These adaptation resources can help reduce vulnerability by providing cooling spaces, healthcare, and financial means to cope with heat. The formula is:

$$HVA = EA + HSA - HAA \tag{13}$$

Where *HVA* represents the heat vulnerability index, a higher value indicates a more severe impact of heat disasters, while a lower value suggests a weaker impact; *HEA* is the heat exposure index; *HSA* is the heat sensitivity index; *HAA* refers to the heat adaptability index. The *HVA* is calculated using Eq. (6), and the natural breaks classification method in ArcGIS Pro is then used to classify heat vulnerability into five levels: high vulnerability risk, relatively high vulnerability risk, medium vulnerability risk, relatively low vulnerability risk, and low vulnerability risk.

3.7. GeoDetector

The GeoDetector method was developed based on two fundamental geographic laws and spatial statistical techniques. It effectively assesses the impact of various influencing factors on the distribution of geographical phenomena [56–58]. This method uses the heat vulnerability index as the dependent variable. It employs factor and interaction detectors to analyse the driving factors of heat vulnerability, exploring the driving force of each factor on heat vulnerability. This model has been widely applied in earth sciences, social sciences, and public health research [59].

3.7.1. Factor detector

The factor detector investigates the influence of individual factors on heat vulnerability [60] and quantifies the extent to which each factor explains the spatial variation in heat vulnerability.

The formula for GeoDetector factor detection is as follows:

$$q = 1 - \frac{\sum_{h=1}^L N_h \sigma_h^2}{N \sigma^2} = 1 - \frac{SSW}{SST} \tag{14}$$

$$SSW = \sum_{h=1}^L N_h \sigma_h^2, \quad SST = N \sigma^2 \tag{15}$$

Where *h* represents the layer number of the independent variable, and *N_h* is the number of sample units in each zone; *N* is the total number of

samples in the entire study area; *L* is the total number of zones (or categories) of the independent variables; and σ_h^2 is the variance within each zone, and σ^2 is the global variance in the entire study area. *SSW* is the variances within the zone; *SST* is the global variance of the dependent variables in the study area. A factor detector can detect whether each potential impact factor is the impact factor of heat vulnerability, with its explanatory power measured by the *q*-value, ranging from [0,1], where a more significant value indicates stronger explanatory power.

3.7.2. Interaction detector

The interaction detector examines the combined effects of pairs of factors on heat vulnerability [61] and determines whether the interaction between two factors enhances or weakens their individual effects on heat vulnerability. The interaction detector evaluates the strength and type of interaction between two factors by calculating their combined *q*-value (*q*(*X1*∩*X2*)) and comparing it with the individual *q*-values (*q*(*X1*) and *q*(*X2*)). Table 3 shows the classification of these interactions. The ID categorizes these interactions into several types: weakening (nonlinear or univariate), enhancing (either bivariate or nonlinear), or independent, based on the relative values of *q*(*X1*), *q*(*X2*), and *q*(*X1*∩*X2*). In this study, the ID is applied to assess whether the interaction of key driving factors, such as NDVI, population density, or socio-economic variables, intensifies or reduces their collective impact on heat vulnerability.

4. Results

4.1. Exposure assessment

The city of Guangzhou has been divided into five levels of heat exposure risk: extremely high risk (0.723–1.000), high risk (0.605–0.722), moderate risk (0.511–0.604), low risk (0.389–0.510), and extremely low risk (0.001–0.388) (See Fig. 3 above). Areas with higher heat exposure are spread across multiple centres and decrease in intensity from the central to peripheral regions. This phenomenon is primarily attributed to the higher reflection, absorption, and retention of heat in built-up centres, coupled with lower vegetation coverage and weaker heat dissipation capacity, thereby contributing to the heat island effect. High-exposure areas are concentrated in Yuexiu, Liwan, Baiyun, Huadu, Tianhe, and Haizhu and are closely associated with lower greenery in these districts. Panyu exhibits moderate exposure, while southern Conghua experiences lower exposure. Northern Guangzhou registers significantly lower exposure than the south, likely due to higher vegetation coverage on the outer edges, which reduces heat radiation. Additionally, the Pearl River system may contribute to local cooling effects.

Jinan’s heat exposure risk is classified into five levels: extremely high (0.777–1.000), high (0.683–0.776), moderate (0.589–0.682), low (0.464–0.588), and extremely low (0.001–0.463) (See Fig. 3 below). The distribution demonstrates a “high centre, low periphery” pattern. The central urban districts of Tianqiao, Huaiyin, Licheng, and central Lixia face high exposure risks due to concentrated buildings, population, and lower greenery. Laiwu also exhibits high exposure, potentially due to industrial activities, as it serves a significant steel industry base, and emissions from large steel enterprises may contribute to localised heat gains. In contrast, Changqing and southern Lixia have lower exposure

Table 3
Types of interaction relationships between the two factors.

Criterion	Interaction
$q(X1 \cap X2) < \min(q(X1), q(X2))$	Weaken; nonlinear
$\min(q(X1), q(X2)) < \max(q(X1), q(X2))$	Weaken; nonlinear; univariate
$q(X1 \cap X2) > \min(q(X1), q(X2))$	Enhance; bivariate
$q(X1 \cap X2) = q(X1) + q(X2)$	Independent
$q(X1 \cap X2) > q(X1) + q(X2)$	Enhance; nonlinear

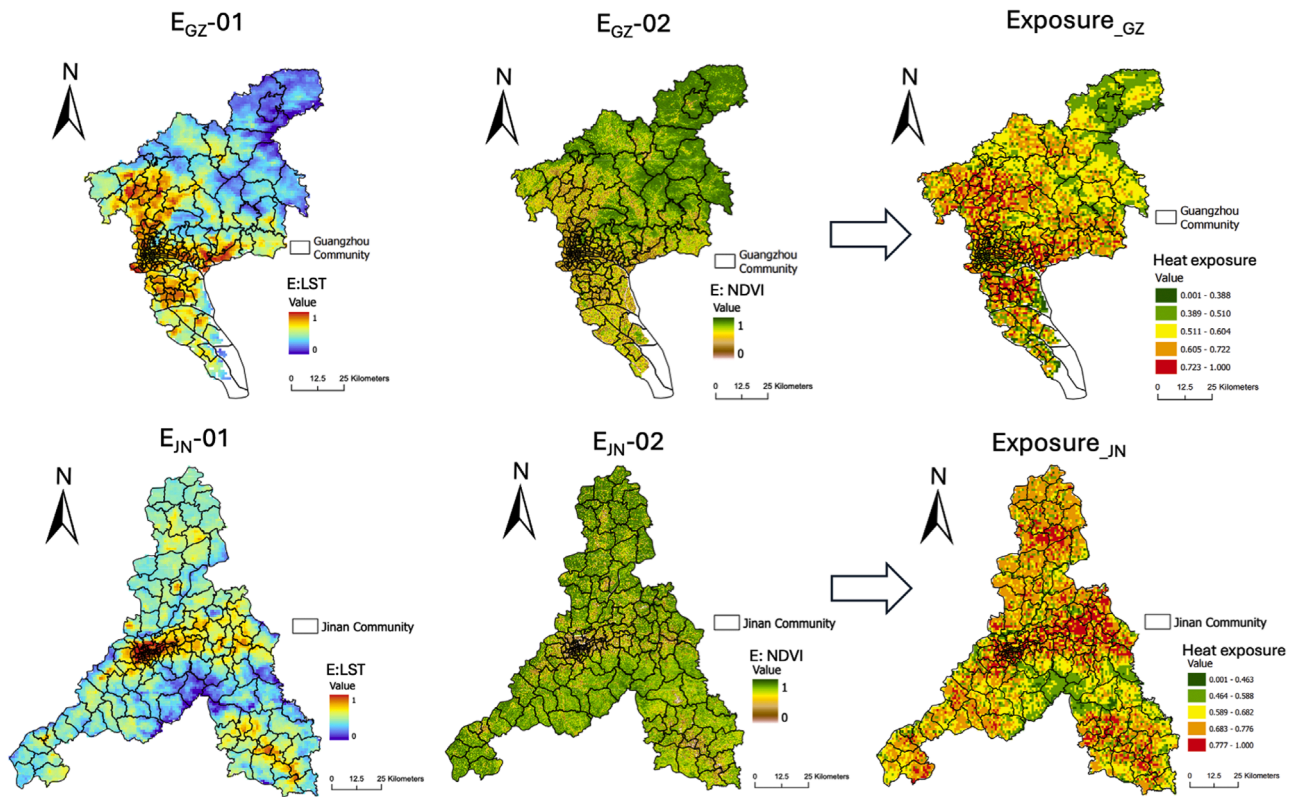


Fig. 3. Spatial distribution of the heat exposure indicators in Guangzhou and Jinan.

risks due to their proximity to forests, highlighting the critical role of vegetation in cooling. Central Shanghe County exhibits moderately high exposure, likely because its northern location in Jinan shields it from cooling southerly winds. The southern mountainous areas of Jinan generally have lower exposure, attributed to their higher elevation and

abundant vegetation cover. The spatial pattern of heat exposure in Jinan reflects the combined effects of urbanisation, terrain, and vegetation while demonstrating the moderating influence of natural geography on thermal environments.

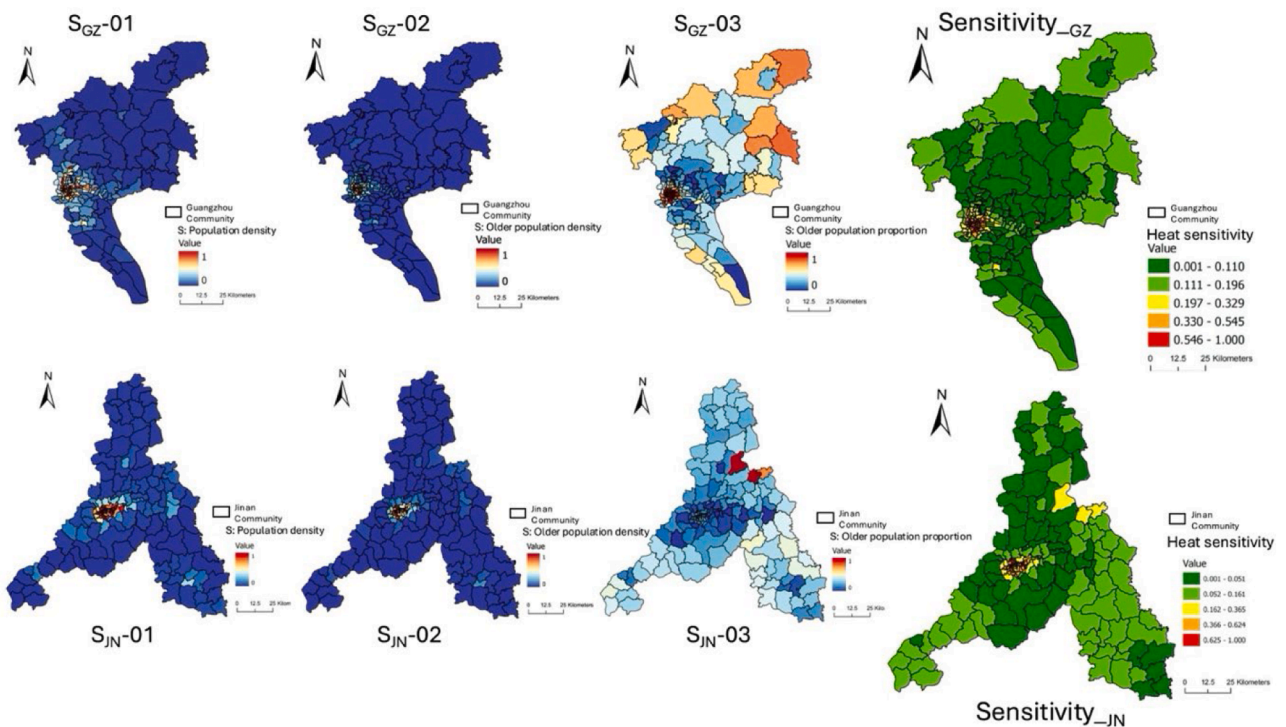


Fig. 4. Spatial distribution of the heat sensitivity indicators in Guangzhou and Jinan.

4.2. Sensitivity assessment

The sensitivity index is determined by calculating a weighted average of three indicators: the proportion of older population, total population density, and older population density. The results of the heat sensitivity assessment are presented in Fig. 4. Sensitivity is classified into five levels using the Jenks natural breaks classification method.

In Guangzhou, sensitivity classes are classified as extremely high risk (0.546–1.000), high risk (0.330–0.545), moderate risk (0.197–0.329), low risk (0.111–0.196), and extremely low risk (0.001–0.110). Areas with high and moderately high risk are primarily located in Yuexiu and Tianhe districts, which are traditional city centres with dense populations, vibrant economic activity, and potentially a higher proportion of older residents. Conversely, areas with lower sensitivity are mainly located in Panyu, Huadu, Zengcheng, Huangpu, and Nansha districts, with relatively lower population densities and proportions of older residents.

In Jinan, sensitivity classes are categorised as extremely high risk (0.625–1.000), high risk (0.366–0.624), moderate risk (0.162–0.365), low risk (0.052–0.161), and extremely low risk (0.001–0.051). The Licheng and Shizhong districts are identified as high-sensitivity areas due to their status as traditional urban cores with dense and ageing populations. The northern Zhangqiu area exhibits moderate sensitivity, which could be linked to its demographic composition.

In both cities, urban centres typically show higher sensitivity due to higher total population densities and the proportions and densities of older residents. The sensitivity index shows a concentric pattern of decreasing risk from urban cores to peripheral areas, closely associated with population distribution characteristics.

4.3. Adaptation assessment

Assessing adaptive capacity involves using an adaptability index, calculated as the weighted average of six indicators: the proportion of the population with a high level of education, the number of hospitals, metro stations, shopping malls, gardens, and per capita disposable income. Subsequently, the adaptability index is classified into five risk levels using the Jenks natural breaks classification method.

In Guangzhou, the risk level is divided into five categories: extremely high risk (0.730–1.000), high risk (0.41–0.729), moderate risk (0.323–0.490), low risk (0.170–0.322), and extremely low risk (0.001–0.169) (Refer to Fig. 5). The adaptive capacity in Guangzhou exhibits a distinct “strong south, weak north” pattern, declining from the southern/central areas towards the north and west. Central districts, such as Tianhe, Yuexiu, and Haizhu, exhibit the strongest adaptability, boosted by higher education institutions, well-established medical facilities, extensive metro networks, numerous shopping malls, ample parks, and higher average disposable incomes. In contrast, the northern and northwestern regions, like Conghua, Huadu, and northern Baiyun, display weaker adaptive capacity, primarily due to their distance from the urban core and relatively lower levels of education, healthcare, public transport, commercial facilities, and potentially lower average incomes. This distribution reflects an unequal allocation of resources and development in Guangzhou.

In Jinan, the risk level is also divided into five classes: extremely high risk (0.621- 1.000), high risk (0.448–0.620), moderate risk (0.295–0.447), low risk (0.142–0.294), and extremely low risk (0.001–0.141) (See Fig. 6). The adaptability in Jinan follows a concentric pattern, originating from the city centre and diminishing towards the periphery, especially in the northeast and southwest. The central districts of Shizhong, Licheng, and central Huaiyin demonstrate the

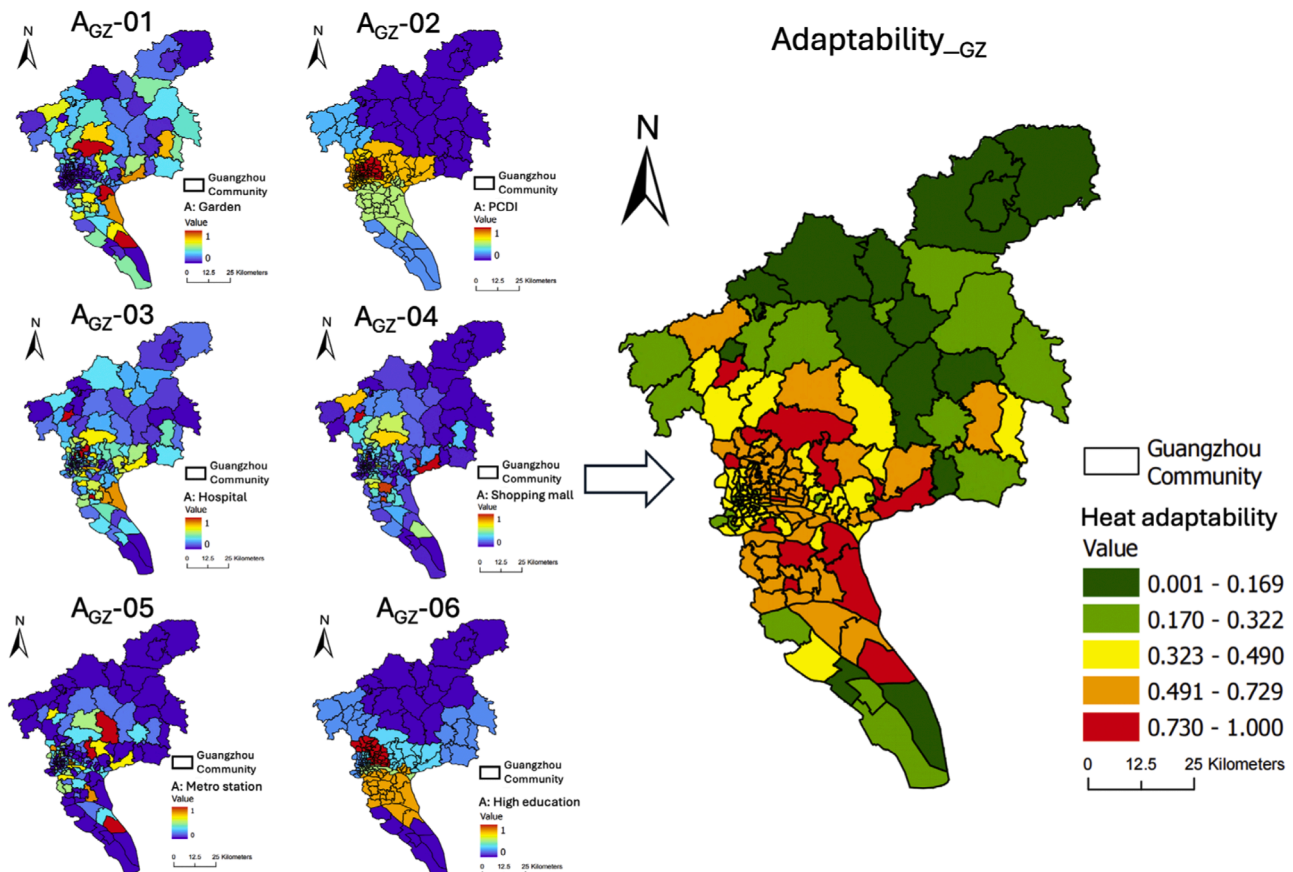


Fig. 5. Spatial distribution of adaptation ability in Guangzhou.

highest resilience, supported by a strong presence of higher education institutions, concentrated hospital facilities, an improving metro system, major commercial centres, ample parks, and higher average disposable incomes. Conversely, peripheral areas, such as Changqing, Zhangqiu, and Jiyang, exhibit weaker adaptive capacity due to their distance from downtown and relative lack of higher education, healthcare, infrastructure, and public services. This pattern underscores the developmental gap between Jinan's urban core and peripheral regions.

4.4. Vulnerability assessment

The heat vulnerability risk index was calculated based on exposure, sensitivity, vulnerability factors, and their respective weights. Subsequently, it was categorised into five levels using the Jenks natural breaks classification method. The spatial distribution of the heat vulnerability risk levels in Jinan and Guangzhou was then obtained (refer to Fig. 7).

In Guangzhou, South China's economic, cultural, and transportation hub, there are notable geographic differences in urban vulnerability. Core districts, like Haizhu and Liwan, have lower vulnerability due to their robust infrastructure, abundant medical resources, developed public transit systems, and extensive green space coverage. Residents in these areas also enjoy higher incomes and robust social services, which enhance their adaptive capacity to external shocks. However, some older neighbourhoods in central districts, like Yuexiu and Tianhe, face higher vulnerabilities due to dense construction, ageing populations, and complex legacy issues. Peripheral districts, like Conghua and Zengcheng, exhibit higher vulnerabilities due to relatively slower urbanisation, unequal distribution of public resources, inadequate public transit networks, and lower economic development. Disasters, economic fluctuations, and other external disturbances may impact these areas. Additionally, rapidly developing districts, like Panyu and Nansha, display medium vulnerability, reflecting rapid population growth and imbalances in infrastructure development. Prioritising sustainable development, optimised resource allocation, and environmental protection could mitigate future risks in these emerging districts.

In Guangzhou, South China's economic, cultural, and transportation hub, there are notable geographic differences in urban vulnerability. Core districts, like Haizhu and Liwan, have lower vulnerability due to their robust infrastructure, abundant medical resources, developed public transit systems, and extensive green space coverage. Residents in these areas also enjoy higher incomes and robust social services, which enhance their adaptive capacity to external shocks. However, some older neighbourhoods in central districts, like Yuexiu and Tianhe, face higher vulnerabilities due to dense construction, ageing populations, and complex legacy issues. Peripheral districts, like Conghua and Zengcheng, exhibit higher vulnerabilities due to relatively slower urbanisation, unequal distribution of public resources, inadequate public transit networks, and lower economic development. Disasters, economic fluctuations, and other external disturbances may impact these areas. Additionally, rapidly developing districts, like Panyu and Nansha, display medium vulnerability, reflecting rapid population growth and imbalances in infrastructure development. Prioritising sustainable development, optimised resource allocation, and environmental protection could mitigate future risks in these emerging districts.

In Jinan, the provincial capital of Shandong, there are variations in urban vulnerability across different districts. Core districts, such as Licheng, Shizhong, Tianqiao, and central Changqing, have lower vulnerability due to their higher economic development, ample medical and educational resources, well-established public transit, and modern infrastructure, making them more resilient against various risks. However, peripheral regions, like Shanghe County, northern Zhangqiu, and Pingyin County, have higher vulnerabilities due to relatively weaker economies, inadequate healthcare, poor transportation, ageing populations, and limited educational resources, making them more susceptible to external shocks, such as economic fluctuations or disasters. Additionally, some Huaiyin and Lixia districts face medium vulnerability due to the slow redevelopment of old communities and high population density during urbanisation. It is crucial to prioritise improving living conditions and enhancing resilience in these communities.

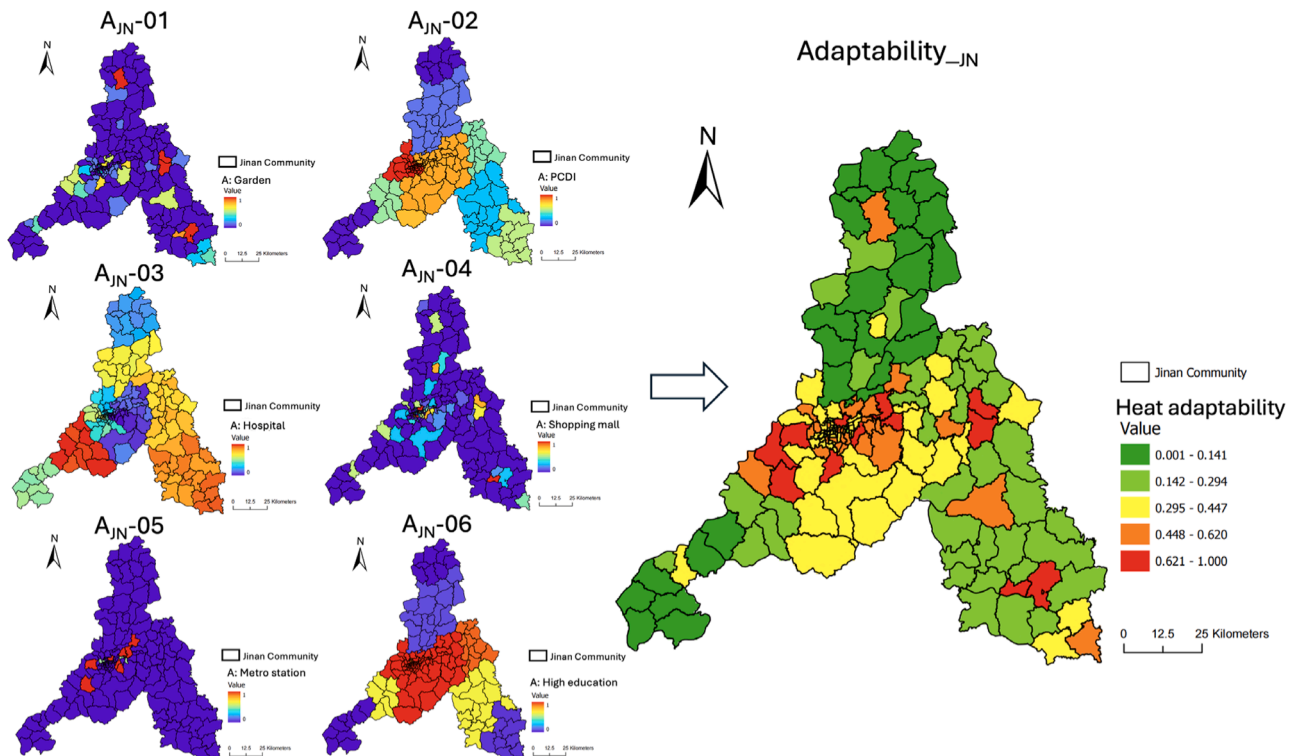


Fig. 6. Spatial distribution of adaptation ability in Jinan.

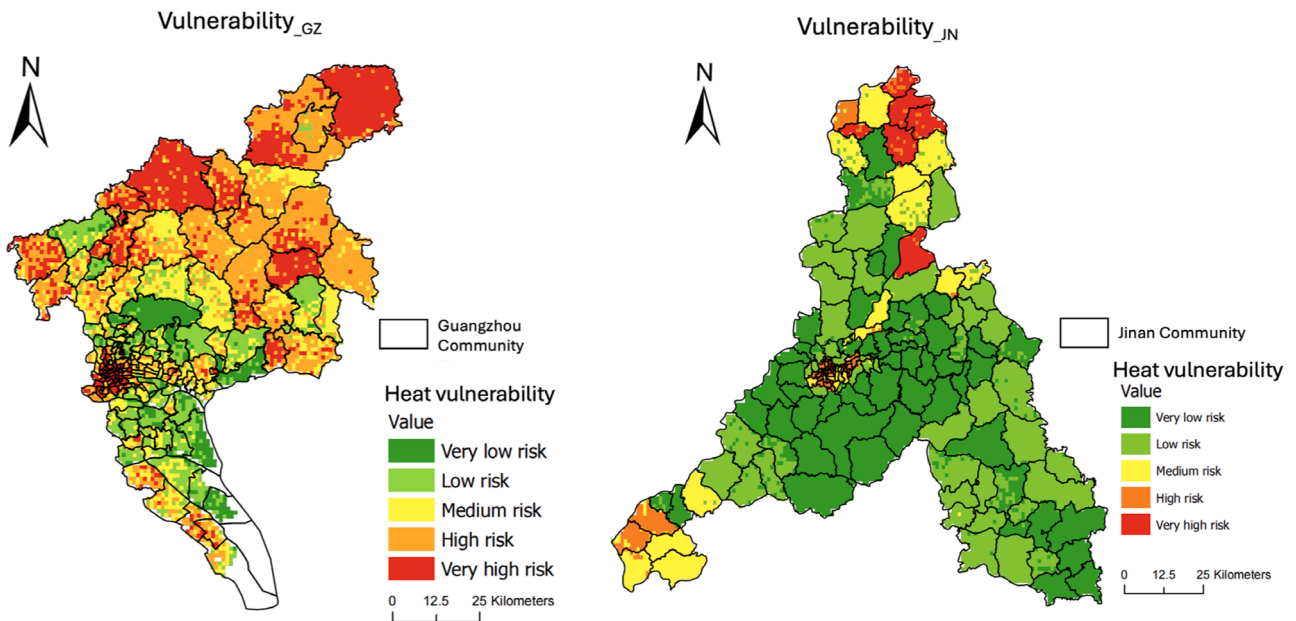


Fig. 7. Distribution of the heat vulnerability risks in Guangzhou (left) and Jinan (right).

The study identifies vulnerability risks at a finer community scale by examining the spatial distribution of heat vulnerability risk. The Ridgeline Plot indicates the presence of multiple high-risk communities with vulnerability values exceeding 90 % in both cities. In Guangzhou, areas such as Beijing, Binjiang, Changang, Chongqing, Datang, Guangta, Haichuang, Huadi, and Hualin are identified as high-risk communities (see Fig. 8). Similarly, in Jinan, communities including Guanzhaying, Hongjialou, Huairen, Huanghe, and Qilishan are also found to face

severe heat risks, characterised by high exposure and sensitivity (see Fig. 9).

4.5. Factors driving heat vulnerability

The results of the GeoDetector analysis reveal the main factors influencing heat vulnerability. In Jinan, the proportion of the older population has the strongest explanatory power, with a q-statistic value

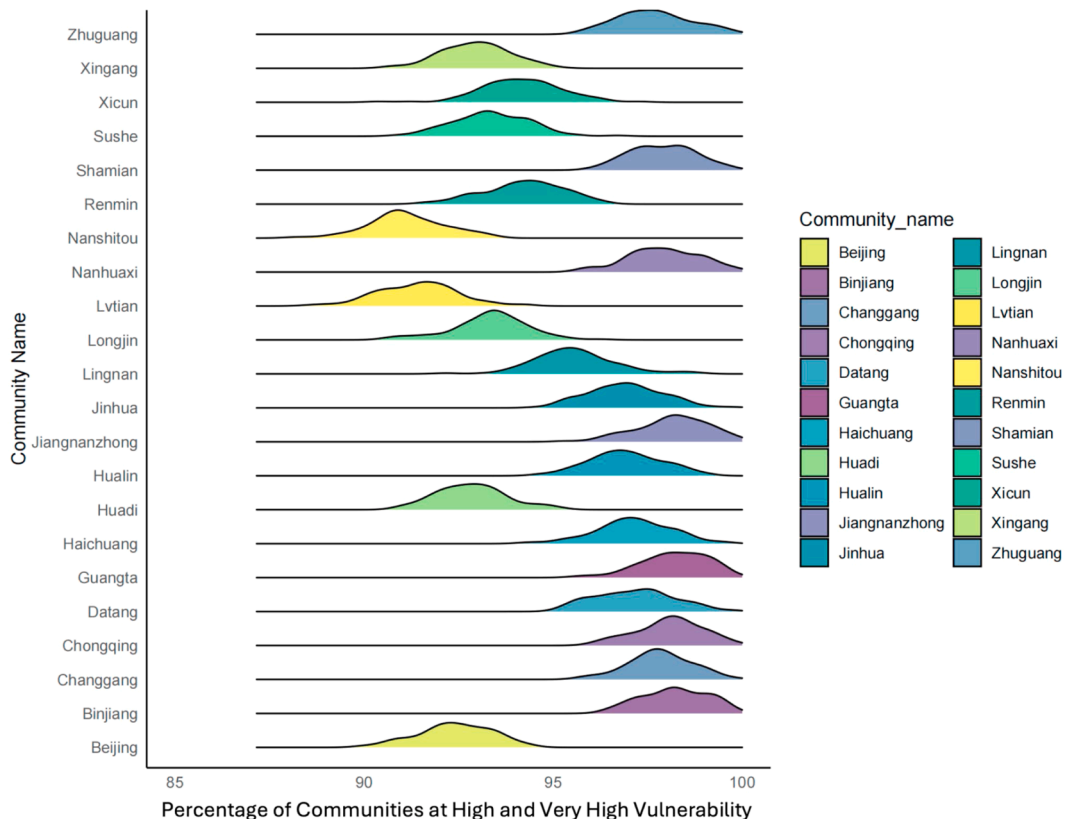


Fig. 8. High and Very High Vulnerability Levels (Above 90 %) in Guangzhou’s Communities.

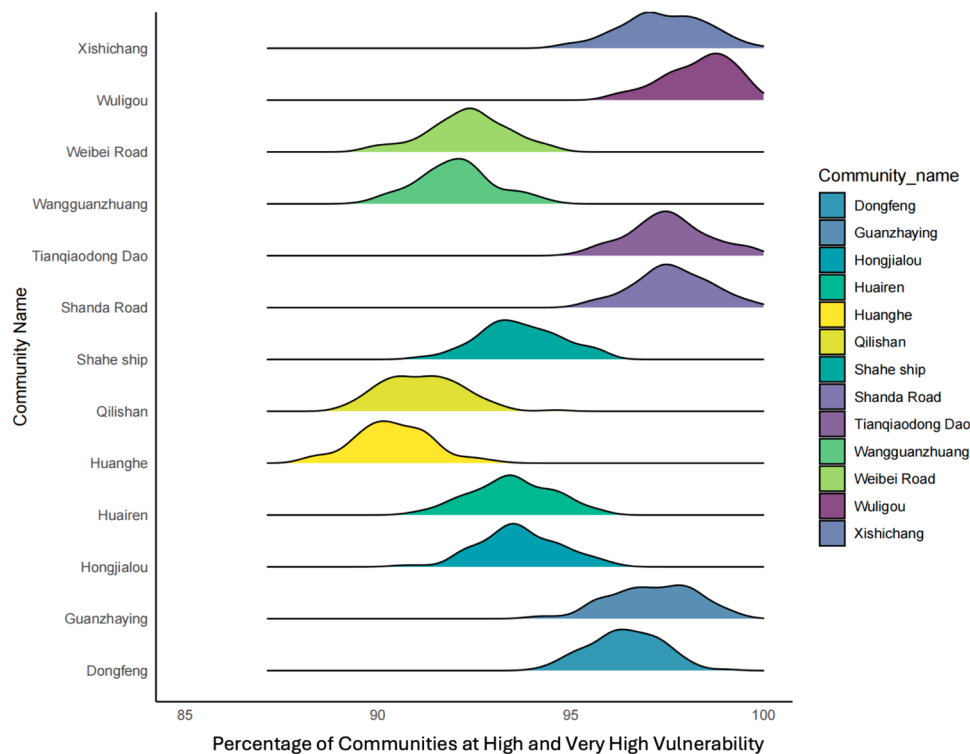


Fig. 9. High and Very High Vulnerability Levels (Above 90 %) in Jinan's Communities.

of 0.2899, indicating its crucial role in heat vulnerability (Table 4). Older individuals are more susceptible to heat waves due to their physiological characteristics, which make them less adaptable and resistant to extreme heat.

In Guangzhou, higher education emerges as the most significant factor, with a q statistic of 0.3257, suggesting that educational level is pivotal in mitigating heat vulnerability (Table 4). Highly educated populations may have better access and understanding of heat protection measures, enabling them to cope more effectively with high-temperature events. This finding underscores the significance of education in enhancing community resilience to heat-related risks.

In Jinan, the higher proportion of the older population emerges as a significant contributing factor to heat vulnerability, supported by a notable impact (q-statistic of 0.2961). The older population may face elevated health risks during high temperatures. The total population density (q-statistic of 0.2440) follows closely, which may exacerbate the urban heat island effect, thereby increasing heat vulnerability.

Additionally, NDVI demonstrates a substantial influence (q-statistic of 0.2440), reflecting the positive role of urban greenery in mitigating heat vulnerability. In contrast, the presence and distribution of metro stations have the most negligible impact on heat vulnerability (q-statistic of 0.0023), suggesting that while Jinan's metro system offers

Table 4

The q statistic of the factor detector ($p = 0$) in Jinan and Guangzhou.

Indicator	q statistic (Jinan)	q statistic (Guangzhou)
LST	0.1772	0.1490
NDVI	0.2440	0.1644
Total population density	0.2961	0.0899
Older population density	0.2099	0.0890
Older population proportion	0.2899	0.2630
Garden	0.0128	0.2545
Metro	0.0023	0.0232
PCDI	0.0819	0.2448
Hospital	0.0840	0.1127
Shopping mall	0.0202	0.1402
High-level education	0.0570	0.3257

convenient transportation for residents, its direct contribution to mitigating environmental heat stress may be limited.

In Guangzhou, the level of education among the population has the most significant impact on heat vulnerability (q-statistic of 0.3257), potentially indicating an association between education level and the ability of urban residents to cope with heat-related disasters. Following this, the proportion of the older population (q-statistic of 0.2630) and PCDI (q-statistic of 0.2448) suggest that the older demographic and economic conditions are also crucial factors influencing heat vulnerability in Guangzhou. Like Jinan, the impact of subway stations on Guangzhou's heat vulnerability is relatively small (q-statistic of 0.0232), further corroborating the indirect nature of subway systems in reducing heat vulnerability. While individual factors have distinct impacts on the environment, the interaction of multiple factors provides a more intuitive exploration of the driving forces behind heat vulnerability in both regions.

4.5.1. Interaction detector analysis

Multi-Factor Drivers of Heat Vulnerability in Guangzhou

Guangzhou's interaction analysis reveals strong connections between education levels and other factors, particularly green spaces ($q = 0.522$), PCDI ($q = 0.352$), and older population densities ($q = 0.481$) (see Fig. 10). Areas with higher education levels in Guangzhou often coincide with better infrastructure, potentially reducing heat vulnerability. However, the strong interaction with older population density suggests that even well-resourced areas face challenges from demographic ageing.

PCDI demonstrates significant interaction effects with different factors, especially green space ($q = 0.508$) and the proportion of the older population ($q = 0.476$). These findings suggest that economic conditions play a crucial role in shaping the distribution of urban greenery and the resilience of older residents. Wealthier areas tend to have more green space, which can help mitigate the heat island effect.

Another notable finding is the interaction between hospital resources and green space ($q = 0.505$). This suggests that integrating healthcare facilities with green areas is crucial in Guangzhou's urban planning to

H1: Two-Factor Interaction Heatmap in Guangzhou

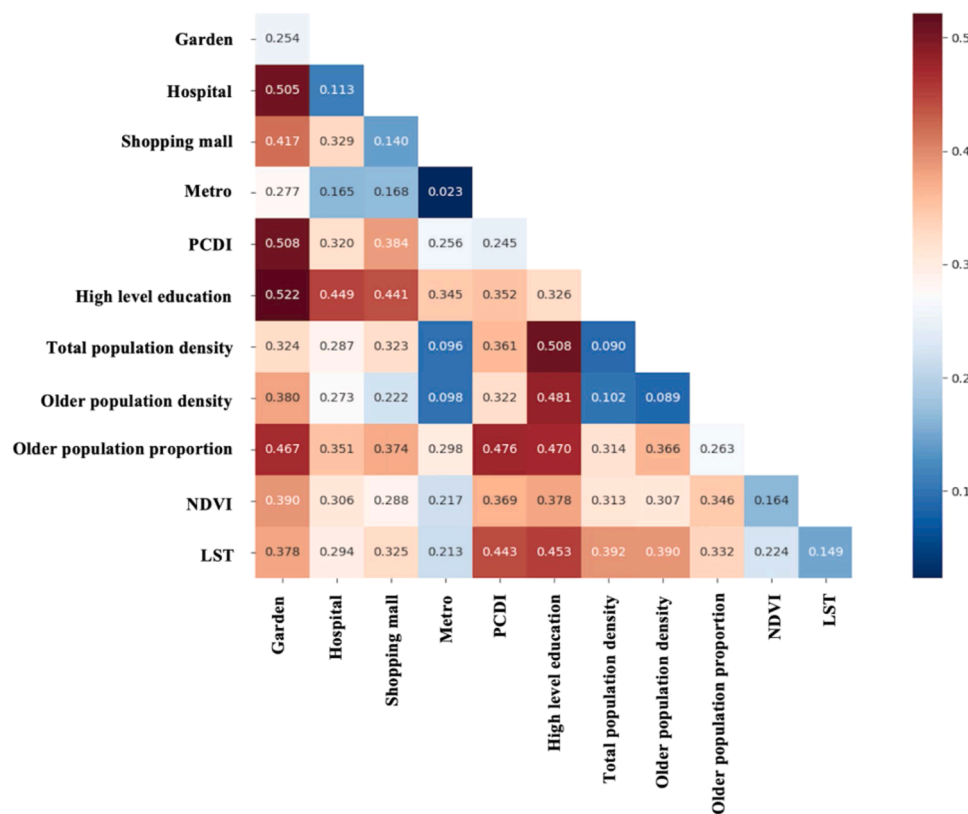


Fig. 10. Effect of two-factor interaction on vulnerability to heat in Guangzhou.

mitigate heat vulnerability. Access to healthcare and urban green spaces can help residents cope with extreme heat, so their combined presence is particularly beneficial in reducing vulnerability.

The interactions between LST and socio-economic factors such as PCDI ($q = 0.443$) and education levels ($q = 0.453$) emphasise the complex relationships between urban heat and social development. Conversely, the metro systems exhibit relatively weak interactions with other factors, likely due to the extensive and well-established metro network in Guangzhou, which minimises variations in its impact on heat vulnerability across different regions. The NDVI shows moderately strong interactions with various factors, reflecting Guangzhou’s identity as a “Flower City,” where urban greening is intricately linked with broader aspects of city development [62].

Guangzhou, as the core engine of the Guangdong-Hong Kong-Macao Greater Bay Area, has undergone rapid urbanisation and economic expansion. Its GDP reached CNY3.04 trillion (USD 4.267 trillion) in 2023, with a permanent population of 10.5661 million [32]. Despite achieving a green coverage rate of 43.6 %, the city still grapples with persistent challenges from the urban heat island effect, with 2023 marking a record number of extreme heat days [33]. This underscores the ongoing need for continued investment in green space and strategic planning to address the ageing population and socio-economic disparities.

Multi-Factor Drivers of Heat Vulnerability in Jinan

The interaction detector analysis for Jinan reveals significant synergistic interactions among population density, older population proportion, and PCDI in contributing to heat susceptibility (See Fig. 11). The interaction between the older population proportion and PCDI is particularly strong ($q = 0.653$), indicating that the combination of economic status and demographic ageing substantially influences heat vulnerability.

Environmental factors like NDVI and LST also interact significantly with population-related factors, highlighting the close relationship between urban greening, heat island effects, and population distribution. While infrastructure factors like metro stations have a relatively small standalone impact, their interaction with population density significantly amplifies their influence on heat vulnerability. This suggests that public transportation may be critical in reducing heat risks in densely populated areas.

The relationship between hospital resources and the density of the older population is particularly significant ($q = 0.426$), emphasising the crucial role of healthcare facility distribution in addressing heat vulnerability, especially within ageing communities. Although education level and shopping centres have limited standalone effects, their influence patterns become more intricate when interacting with economic and population factors.

The findings are closely linked to Jinan’s rapid urbanisation and demographic changes over recent decades. Jinan’s population surged from 1.8 million in 2000 to 9.437 million in 2023, with the proportion of residents aged 60 and above rising from 8.14 % to 23.62 % [29]. This demographic shift and economic development have heightened the city’s vulnerability to extreme heat, particularly in areas with concentrated older and economically disadvantaged populations. Recognising these challenges, Jinan has increased its green coverage from 37.04 % in 2010 to 47.2 % in 2023 [29]. This aligns with our findings on NDVI’s significant role in mitigating heat vulnerability and addressing the environmental pressures caused by rapid urban expansion.

H2: Two-Factor Interaction Heatmap in Jinan

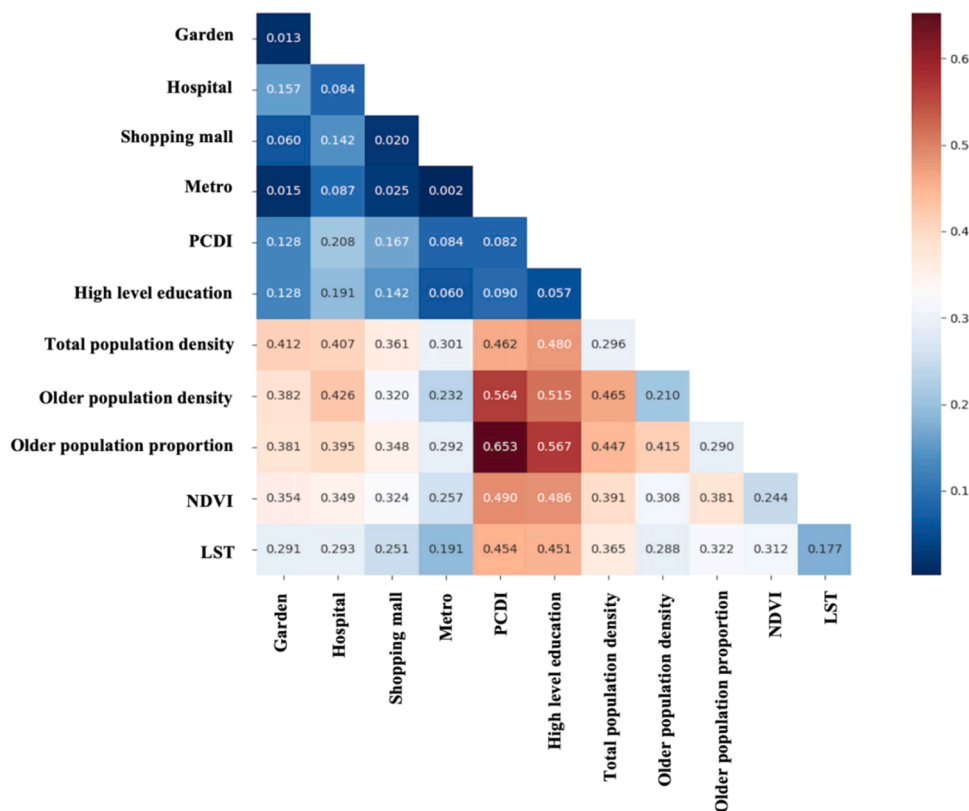


Fig. 11. Effect of two-factor interaction on vulnerability to heat in Jinan.

5. Discussion

5.1. Key factors affecting heat vulnerability

This study employed the GeoDetector model to evaluate heat vulnerability risk among older populations in Guangzhou and Jinan based on the exposure-sensitivity-vulnerability-adaptation framework. The results revealed significant geographical differences in the factors influencing heat vulnerability between these two cities. In Guangzhou, education level emerged as the most influential factor, while in Jinan, the proportion of the older population had the most significant impact. These findings highlight the complex interplay of various elements in shaping urban heat vulnerability.

Education emerged as the most influential factor in Guangzhou, consistent with previous studies linking higher educational attainment to improved risk perception and adaptive capacity [63,64]. Individuals with higher education are better equipped to access information, understand risks, and engage in adaptive behaviours. However, this finding also highlights the risk of exacerbating social disparities due to unequal access to education [65–67]. To address this, future research should explore community-based programs and public awareness campaigns targeting less-educated populations to enhance their heat adaptation capabilities.

Environmental factors, particularly the Normalized Difference Vegetation Index (NDVI), played a significant role in both cities. In Guangzhou, NDVI interacted strongly with per capita disposable income (PCDI) and the proportion of older populations, underscoring the importance of urban greening in mitigating the urban heat island effect [68,69]. However, the unequal distribution of green infrastructure, as highlighted by the concept of “green gentrification” [70], can exacerbate social inequalities. Therefore, the equitable distribution of green spaces in lower-income areas should be a priority in urban planning to

ensure that all residents benefit from greening initiatives.

The interaction between medical facilities and green spaces in Guangzhou underscores the need to integrate public health considerations into environmental planning. Previous studies have shown that access to medical resources can reduce heat vulnerability during heat waves [71]. However, the concentration of hospital resources in affluent green areas risks deepening health inequalities [72]. Policies should aim to decentralize healthcare infrastructure and improve access in vulnerable communities.

In Jinan, the older population emerged as the most influential factor, aligning with global research on the heightened vulnerability of older adults to extreme heat [73,74]. Older adults face physiological and social challenges that increase their risk, emphasising the need for “age-friendly city” concepts [75]. Findings also revealed interactions between income levels and older populations, highlighting the compound impact of socioeconomic inequalities on heat vulnerability [76]. Targeted interventions, such as financial support and community-based cooling initiatives for low-income older residents, are essential to address these challenges.

Building on this socioeconomic dimension of heat vulnerability, Lanza et al. [77] highlighted that low-income older adults often reside in areas disproportionately affected by extreme heat and lack the necessary resources to cope. This aligns with our findings and emphasises the need for targeted interventions in areas with high concentrations of low-income older residents. Owen [78] further emphasised the importance of comprehensively considering socioeconomic factors, demographic characteristics, and environmental conditions in effective climate adaptation strategies. The significant differences between Guangzhou and Jinan underscore the need for tailored and location-specific adaptation strategies for local demographic and socioeconomic conditions. To effectively address the challenges posed by extreme heat, it is necessary to simultaneously address the distribution

of educational resources, green space planning, support for the welfare of older populations, and economic inequalities.

5.2. Community characteristics and heat vulnerability risk

The spatial disparities of heat vulnerability identified in this study exhibit both consistencies and differences with previous research. Studies highlighted that urban areas with higher heat vulnerability are often concentrated in older neighbourhoods and economically disadvantaged communities [79–81]. This aligns with the distribution of extreme heat vulnerability observed in Guangzhou, where high-risk communities such as Beijing, Binjiang, Changgang, Chongqing, Datang, Guangta, Haichuang, Huadi, and Hualin are typically located in the city centre or underdeveloped peripheral areas. Notably, the study found that Guangzhou's high heat vulnerability is not only clustered in the older districts of the urban centre but also extends to some peripheral regions that are underdeveloped and lack adequate infrastructure. Similarly, in Jinan, areas with high vulnerability—such as Guanzhaying, Hongjialou, Huairan, Huanghe, and Qilishan—are primarily situated in socioeconomically disadvantaged peripheral counties with insufficient services. This pattern is consistent with previous research, which identified clusters of heat vulnerability in urban centres and suburban edges [82,83]. Therefore, more attention must be paid to this community type during heat waves.

The Associations between community characteristics and heat vulnerability risk suggest that our findings are broadly applicable. They extend beyond the heat-prone areas examined in this study to other cities affected by heat waves, particularly those with similar development levels and geographic conditions. Further research could validate and extend these results across diverse cities and regions, particularly in urban areas grappling with rapid growth, ageing populations, and rising temperatures.

5.3. Applicability of heat vulnerability assessment model

Urban areas' vulnerability to heat is shaped by environmental, socio-economic, and cultural factors [61]. Although progress has been made in developing heat vulnerability assessment models, urban heat dynamics are often oversimplified. This oversimplification reflects a fundamental misunderstanding of urban heat vulnerability rather than a methodological shortcoming.

Current models generally fall into two categories, each with limitations. Environmental-focused models (e.g., Yin et al. [84]; Kershaw and Millward [85]) effectively identify physical hazards but often disregard social vulnerability factors, assuming uniform human responses to heat stress. Conversely, socially focused models (e.g., Barron et al. [86]) address demographic and socio-economic disparities but overlook physical aspects such as urban heat island effects or access to green infrastructure. This methodological divide limits the utility of these models in urban planning and public health strategies, highlighting the need for an integrated, systems-thinking approach.

Our study emphasizes the importance of a holistic framework that integrates environmental, social, economic and infrastructural factors. For example, our inclusion of NDVI as an exposure indicator represents a step forward compared to prior studies relying solely on temperature metrics like LST [87]. Additionally, adaptation indicators such as metro systems, hospitals, and shopping centres provide a fresh perspective on urban heat resilience. However, further validation is required to assess these indicators' broader applicability and effectiveness.

A critical challenge in heat vulnerability assessment lies in the inconsistent classification of indicators. For instance, while this study categorizes the older population as part of sensitivity, other research (e.g., [88,89]) classifies it as an exposure indicator. Similarly, we use PCDI instead of GDP as an economic indicator to reflect a more nuanced understanding of individual adaptive capacity, contrasting with studies like Lim et al. [90] that categorise GDP as a sensitivity metric. These

discrepancies underscore the urgent need for standardisation in selecting and classifying indicators to ensure comparability across studies and to strengthen policy relevance.

Moving forward, developing more comprehensive models integrating environmental, social, and infrastructural factors while working towards a more standardised approach to indicator selection and classification is necessary. Through such holistic and standardised assessment, we can fully understand and effectively address the complex challenges of urban heat vulnerability in rapidly urbanising cities.

5.4. How to reduce the heat vulnerability of older people to improve community climate resilience?

While the ageing population mainly affects Jinan's heat vulnerability, Guangzhou is exacerbated by socio-economic disparities and rapid urbanisation in its peripheral regions. We propose the following community heat vulnerability adaptation strategies based on the distribution of heat vulnerability.

For Guangzhou:

- 1) Improving the urban built environment by adopting green infrastructure and reflective materials is essential for reducing heat exposure in Guangzhou. Specific initiatives can include installing vertical gardens on building facades, creating rooftop greenery, and increasing street-level vegetation such as shaded walkways and tree-lined streets.
- 2) The retrofitting of ageing residential buildings must be prioritised to address the risks of extreme heat, particularly for vulnerable groups like older adults and low-income residents. Key upgrades include applying reflective coatings or materials to building exteriors to reduce heat absorption and improve indoor thermal conditions.
- 3) Increasing green space coverage is essential for improving urban microclimates and reducing neighbourhood-level heat exposure. Converting underutilised urban spaces or vacant lots into pocket parks, for instance, can expand green coverage even in densely built-up neighbourhoods.
- 4) Public awareness campaigns can disseminate information about heat-related health risks and help residents recognise warning signs of heat exhaustion or heatstroke. Outreach initiatives could include distributing brochures, holding workshops, and leveraging digital platforms such as apps or social media to share real-time heat alerts and safety tips. For example, creating a city-wide "Heatwave Week" with interactive activities and expert seminars could engage residents and encourage proactive heat risk management.

For Jinan:

- 1) Community centres can be repurposed as dedicated cooling hubs during heatwaves, providing safe, air-conditioned spaces for vulnerable populations, particularly older adults. These hubs can have cooling equipment such as fans, air purifiers, and hydration stations to ensure a comfortable indoor environment. Beyond serving as a refuge from extreme heat, these centres can host health education workshops, wellness check-ups, and social events that promote awareness of heat-related risks and foster a sense of community.
- 2) Providing health monitoring devices tailored to older adults can enable real-time tracking of vital signs such as body temperature, heart rate, and hydration levels during heatwaves. These devices, such as wearable smartwatches or sensor-based trackers, could automatically alert caregivers or healthcare professionals when abnormal readings are detected, ensuring timely medical intervention. For example, if an older person's body temperature reaches a critical threshold, the system could immediately notify emergency services or family members. Integrating these devices into the community healthcare system would allow local clinics or health centres to maintain a centralised database for proactive monitoring.

- 3) Strengthening community healthcare services is essential to address heat-related health risks effectively. Increasing the number of healthcare workers, particularly during heatwaves, can ensure that at-risk populations like older people receive timely and effective care. Community health workers should be trained to recognise signs of heat-related illnesses, such as dehydration, heat exhaustion, and heatstroke, and to provide immediate assistance or referrals to higher-level care.
- 4) Building age-friendly communities by proactively establishing heat emergency response teams can help monitor older residents' living conditions and well-being through regular phone check-ins, home visits, and cooling supply distribution. Additionally, community-led health education campaigns can raise residents' heat risk awareness and self-protection capabilities.

6. Conclusion

This study developed an innovative model for assessing urban heat vulnerability by integrating exposure, sensitivity, and adaptive capacity into a comprehensive framework. The model incorporates key indicators, such as LST, NDVI, and adaptation resources like metro access, hospitals, and PCID, to provide a nuanced understanding of vulnerability. By leveraging GeoDetector, the model effectively identifies key factors influencing heat vulnerability, including the interactions between environmental, demographic, and adaptive components, and offers actionable insights for urban planning and policy development. Our research showed that education level emerged as the most critical factor in Guangzhou, reflecting its role in enhancing risk perception and adaptive capacity. In contrast, Jinan's heat vulnerability was primarily driven by the proportion of older populations, underscoring the heightened risks ageing communities face.

Focusing on the community-scale level for a finer-grained analysis enables identifying urban hotspots (e.g., high-risk areas in Jinan and Guangzhou, as shown in the Results). This approach provides crucial support for guiding heat stress mitigation measures, particularly by enhancing the adaptive capacity of local communities. High-risk communities in both cities were concentrated in socioeconomically disadvantaged areas, including older urban centres and underdeveloped peripheral zones. These findings emphasise the need for targeted interventions to reduce vulnerability in such areas.

It is crucial to acknowledge the limitations inherent in this study. Primarily, the research exclusively examines the summer of 2023, thereby constraining the ability to capture temporal changes or seasonal variations in urban heat vulnerability. Additionally, while the focus on Guangzhou and Jinan facilitates an in-depth analysis, the findings may not be wholly generalisable to other urban environments. These cities exhibit unique climatic conditions, socio-economic structures, and urban development patterns distinct from those found in regions characterised by diverse cultural, geographical, or climatic attributes.

Moreover, despite conducting a comprehensive literature review to guide the selection of indicators, certain relevant factors remain underexplored due to constraints in available data. For instance, the potential influence of other vulnerable populations, such as children, as well as housing conditions and access to green spaces, could significantly impact adaptive capacity and exposure to heat stress. Unfortunately, these crucial aspects were not adequately addressed within the scope of this study.

Upcoming research may utilise dynamic and temporal datasets to elucidate seasonal variations and long-term trends in heat vulnerability. Such an approach will facilitate real-time updates and yield more precise risk assessments. By extending the scope of the study to encompass diverse urban contexts, including cities in South Asia, Southeast Asia, Africa, the Middle East, and Latin America, its applicability is enhanced and valuable insights are provided into varying socio-economic and environmental conditions.

Enhancing data collection remains paramount. This can be done by

incorporating high-resolution thermal imagery, comprehensive demographic surveys, and meticulous green space mapping to refine vulnerability assessments. Furthermore, future research should prioritise the tracking and forecasting of urban transformations, including demographic shifts, advancements in educational attainment, income disparities, and infrastructure development. This focus will enable the design of resilient and adaptive strategies that respond effectively to the evolving urban landscape.

Moreover, addressing gaps in indicator selection—particularly concerning children's vulnerability, housing quality, and access to cooling infrastructure—will contribute to a more robust understanding of adaptive capacity. Ultimately, developing heat vulnerability risk maps will be essential for governments and urban planners. These maps will assist in implementing targeted strategies at the community level, effectively addressing extreme heat, bolstering adaptive capacity, and safeguarding vulnerable populations.

Funding

None to report.

CRedit authorship contribution statement

Jifei Chen: Writing – review & editing, Writing – original draft, Visualization, Methodology, Formal analysis, Data curation, Conceptualization. **Xiaoming Shi:** Writing – review & editing, Writing – original draft, Validation. **Yongying Shi:** Conceptualization. **Laurence L. Delina:** Writing – review & editing, Writing – original draft, Supervision, Conceptualization.

Declaration of competing interest

The authors declare that they have no known competing financial interests or personal relationships that could have appeared to influence the work reported in this paper.

Supplementary materials

Supplementary material associated with this article can be found, in the online version, at [doi:10.1016/j.buildenv.2025.112622](https://doi.org/10.1016/j.buildenv.2025.112622).

Data availability

Data will be made available on request.

References

- [1] ... & A. AghaKouchak, F. Chiang, L.S. Huning, C.A. Love, I. Mallakpour, O. Mazdiyasi, M. Sadegh, Climate extremes and compound hazards in a warming world, *Annu. Rev. Earth Planet. Sci.* 48 (1) (2020) 519–548.
- [2] Y. Wang, N. Zhao, C. Wu, J. Quan, M. Chen, Future population exposure to heatwaves in 83 global megacities, *Sci. Total Environ.* 888 (2023) 164142.
- [3] T.K. Matthews, R.L. Wilby, C. Murphy, Communicating the deadly consequences of global warming for human heat stress, *Proc. Natl Acad. Sci.* 114 (15) (2017) 3861–3866.
- [4] Q. Han, S. Sun, Z. Liu, W. Xu, P. Shi, Accelerated exacerbation of global extreme heatwaves under warming scenarios, *Int. J. Climatol.* 42 (2022) 5430–5441.
- [5] Z. Dong, L. Wang, P. Xu, J. Cao, R. Yang, Heatwaves similar to the unprecedented one in summer 2021 over Western North America are projected to become more frequent in a warmer world, *Earth's Future* (2023) 11.
- [6] S. Russo, A. Marchese, J. Sillmann, G. Immé, When will unusual heat waves become normal in a warming Africa? *Environ. Res. Lett.* (2016) 11.
- [7] C. Park, J. Thorne, S. Hashimoto, D. Lee, K. Takahashi, Differing spatial patterns of the urban heat exposure of elderly populations in two megacities identifies alternate adaptation strategies, *Sci. Total Environ.* (2021).
- [8] Z. Li, X. Guo, Y. Yang, Y. Hong, Z. Wang, L. You, Heatwave trends and the population exposure over China in the 21st century as well as under 1.5 C and 2.0 C global warmer future scenarios, *Sustainability* 11 (12) (2019) 3318.
- [9] C. Faurie, B.M. Varghese, J. Liu, P. Bi, Association between high temperature and heatwaves with heat-related illnesses: a systematic review and meta-analysis, *Sci. Total Environ.* 852 (2022) 158332.

- [10] ... & F.S. Arsad, R. Hod, N. Ahmad, R. Ismail, N. Mohamed, M. Baharom, F. Tangang, The impact of heatwaves on mortality and morbidity and the associated vulnerability factors: a systematic review, *Int. J. Environ. Res. Public Health* 19 (23) (2022) 16356.
- [11] T. Kapwata, M.T. Gebreslasie, C.Y. Wright, An analysis of past and future heatwaves based on a heat-associated mortality threshold: towards a heat health warning system, *Environ. Health* 21 (1) (2022) 112.
- [12] ... & J. Liu, J. Qi, P. Yin, W. Liu, C. He, Y. Gao, M. Zhou, Rising cause-specific mortality risk and burden of compound heatwaves amid climate change, *Nat Clim Chang* (2024) 1–9.
- [13] ... & S. Lobanov-Rostovsky, Q. He, Y. Chen, Y. Liu, Y. Wu, Y. Liu, E.J. Brunner, Growing old in China in socioeconomic and epidemiological context: systematic review of social care policy for older people, *BMC Public Health* 23 (1) (2023) 1272.
- [14] M. Itani, N. Ghaddar, K. Ghali, A. Laouadi, Bioheat modeling of elderly and young for prediction of physiological and thermal responses in heat-stressful conditions, *J. Therm. Biol.* 88 (2020) 102533.
- [15] ... & S. Sun, L. Tian, H. Qiu, K.P. Chan, H. Tsang, R. Tang, C.M. Wong, The influence of pre-existing health conditions on short-term mortality risks of temperature: evidence from a prospective Chinese elderly cohort in Hong Kong, *Environ. Res.* 148 (2016) 7–14.
- [16] J. Wolf, W.N. Adger, I. Lorenzoni, V. Abrahamson, R. Raine, Social capital, individual responses to heat waves and climate change adaptation: an empirical study of two UK cities, *Glob. Environ. Chang.* 20 (1) (2010) 44–52.
- [17] Y. Chen, X. Qin, The impact of extreme temperature shocks on the health status of the elderly in China, *Int. J. Environ. Res. Public Health* 19 (23) (2022) 15729.
- [18] A. El-Zein, F.N. Tonmoy, Assessment of vulnerability to climate change using a multi-criteria outranking approach with application to heat stress in Sydney, *Ecol. Indic.* 48 (2015) 207–217.
- [19] K. Hu, X. Yang, J. Zhong, F. Fei, J. Qi, Spatially explicit mapping of heat health risk utilizing environmental and socioeconomic data, *Environ. Sci. Technol.* 51 (3) (2017) 1498–1507.
- [20] ... & N. Stephenne, B. Beaumont, E. Hallot, F. Lenartz, F. Lefebvre, D. Lauwaet, E. Wolff, Exposure and vulnerability geospatial analysis using earth observation data in the city of Liege, Belgium, *ISPRS Annals of the photogrammetry, Remote Sens. Spatial Inf. Sci.* 4 (2017) 149–156.
- [21] Y.J. Kwon, D.K. Lee, Y.H. Kwon, Is sensible heat flux useful for the assessment of thermal vulnerability in Seoul (Korea)? *Int. J. Environ. Res. Public Health* 17 (3) (2020) 963.
- [22] W.Y. Shih, L. Mabon, Understanding heat vulnerability in the subtropics: insights from expert judgements, *Int. J. Disaster Risk Reduction* 63 (2021) 102463.
- [23] W. Puntub, T. Schnitffinke, M. Fleischhauer, J. Birkmann, M. Garschagen, S. Sandholz, M. Wannewitz, Linking science and practice in participatory future-oriented assessment and planning of human heat stress vulnerability in Bonn, Germany, *J. Environ. Plann. Manage.* 66 (9) (2023) 1918–1937.
- [24] ... & C. Wu, W. Shui, Z. Huang, C. Wang, Y. Wu, Y. Wu, D. Zheng, Urban heat vulnerability: a dynamic assessment using multi-source data in coastal metropolis of Southeast China, *Front Public Health* 10 (2022) 989963.
- [25] J. Dong, J. Peng, X. He, J. Corcoran, S. Qiu, X. Wang, Heatwave-induced human health risk assessment in megacities based on heat stress-social vulnerability-human exposure framework, *Landscape Urban Plan.* 203 (2020) 103907.
- [26] S.H. Lo, C.T. Chen, S. Russo, W.R. Huang, M.F. Shih, Tracking heatwave extremes from an event perspective, *Weather and Climate Extremes* 34 (2021) 100371.
- [27] A.K. Dubey, P. Lal, P. Kumar, A. Kumar, A.Y. Dvornikov, Present and future projections of heatwave hazard-risk over India: a regional earth system model assessment, *Environ. Res.* 201 (2021) 111573.
- [28] Jinan Municipal People's Government (2024). Jinan's Geographical Climate. From: <http://www.jinan.gov.cn/col/col24698/index.html>.
- [29] Shandong Provincial Meteorological Bureau (2024). Major weather events in Jinan. From: <http://sd.cma.gov.cn/gslb/jnsqxj/>.
- [30] Jinan Municipal Bureau of Statistics. (2023). Jinan Statistical Yearbook 2023. From: <http://jntj.jinan.gov.cn/col/col27523/index.html>.
- [31] ... & J. Li, X. Xu, J. Yang, Z. Liu, L. Xu, J. Gao, Q. Liu, Ambient high temperature and mortality in Jinan, China: a study of heat thresholds and vulnerable populations, *Environ. Res.* 156 (2017) 657–664.
- [32] Guangdong Provincial Meteorological Bureau (2024). Overview of Guangzhou's economic operation in the first half of 2024. From: https://www.gd.gov.cn/zwgk/sjfb/dssj/content/post_4465196.html.
- [33] Guangzhou Meteorological Bureau (2024). Meteorological data of Guangzhou. From: <http://gd.cma.gov.cn/gzsqxj/>.
- [34] J. Zhou, X. Zhang, W. Tang, L. Ding, J. Ma, X. Zhang, Daily 1-km all-weather land surface temperature dataset for the China's landmass and its surrounding areas, TRIMS LST; 2000-2022, National Tibetan Plateau /Third Pole Environment Data Centre (2021), <https://doi.org/10.11888/Meteoro.tpd.c.271252>. From.
- [35] J. Dong, Y. Zhou, N. You, The 30 m annual maximum NDVI dataset for China from 2000 to 2020 [DB/OL], National Ecosystem Science Data Centre (2021), <https://doi.org/10.12199/nescd.ecodb.rs.2021.012>.
- [36] The 7th National Population Census Communiqué, National Bureau of Statistics of China, 2021. From, http://www.stats.gov.cn/english/pressrelease/202105/t20210511_1817179.html.
- [37] OpenStreetMap, OSM China POI Data 2014-2021 (2022). Retrieved from, <https://open.geovisearth.com/service/resource/79>.
- [38] Guangzhou Municipal Bureau of Statistics, Guangzhou Statistical Yearbook 2023 (2023). From, https://tj.gz.gov.cn/stats_newtjyw/zyxz/tjnjdzza/content/post_9343663.html.
- [39] ... & G. Cissé, R. McLeman, H. Adams, P. Aldunce, K. Bowen, D. Campbell-Lendrum, M.C. Tirado, 2022: health, wellbeing, and the changing structure of communities (2022).
- [40] M. Alemi-Ardakani, A.S. Milani, S. Yannacopoulos, G. Shokouhi, On the effect of subjective, objective and combinative weighting in multiple criteria decision making: a case study on impact optimization of composites, *Expert Syst. Appl.* 46 (2016) 426–438.
- [41] Y. Liu, C.M. Eckert, C. Earl, A review of fuzzy AHP methods for decision-making with subjective judgements, *Expert Syst. Appl.* 161 (2020) 113738.
- [42] O.S. Vaidya, S. Kumar, Analytic hierarchy process: an overview of applications, *Eur. J. Oper. Res.* 169 (1) (2006) 1–29.
- [43] Y. Zhu, D. Tian, F. Yan, Effectiveness of entropy weight method in decision-making, *Math. Probl. Eng.* 2020 (1) (2020) 3564835.
- [44] Y. Chen, J. Yang, R. Yang, X. Xiao, J.C. Xia, Contribution of urban functional zones to the spatial distribution of urban thermal environment, *Build. Environ.* 216 (2022) 109000.
- [45] M. Gascon, M. Girach, D. Martínez, P. Dadvand, A. Valentín, A. Plasència, M. J. Nieuwenhuijsen, Normalized difference vegetation index (NDVI) as a marker of surrounding greenness in epidemiological studies: the case of Barcelona city, in: *Urban Forestry & Urban Green.*, 19, 2016, pp. 88–94.
- [46] J.B. Leite, J.R.S. Mantovani, T. Dokic, Q. Yan, P.C. Chen, M. Kezunovic, Resiliency assessment in distribution networks using GIS-based predictive risk analytics, *IEEE Trans. Power Syst.* 34 (6) (2019) 4249–4257.
- [47] Y. Sun, Y. Li, R. Ma, C. Gao, Y. Wu, Mapping urban socio-economic vulnerability related to heat risk: a grid-based assessment framework by combing the geospatial big data, *Urban Climate* 43 (2022) 101169.
- [48] G.P. Kenny, J. Yardley, C. Brown, R.J. Sigal, O. Jay, Heat stress in older individuals and patients with common chronic diseases, *CMAJ* 182 (10) (2010) 1053–1060.
- [49] ... & W. Ju, R. Zheng, S. Zhang, H. Zeng, K. Sun, S. Wang, J. He, Cancer statistics in Chinese older people, 2022: current burden, time trends, and comparisons with the US, Japan, and the Republic of Korea, *Sci. China Life Sci.* 66 (5) (2023) 1079–1091.
- [50] ... & O. Jay, A. Capon, P. Berry, C. Broderick, R. de Dear, G. Havenith, K.L. Ebi, Reducing the health effects of hot weather and heat extremes: from personal cooling strategies to green cities, *Lancet North Am. Ed.* 398 (10301) (2021) 709–724.
- [51] K. Seong, J. Jiao, A. Mandalapu, Evaluating the effects of heat vulnerability on heat-related emergency medical service incidents: Lessons from Austin, Texas, *Environ. Plann. B: Urban Analyt. City Sci.* 50 (3) (2023) 776–795.
- [52] ... & B.J. He, D. Zhao, K. Xiong, J. Qi, G. Ulpiani, G. Pignatta, P. Jones, A framework for addressing urban heat challenges and associated adaptive behavior by the public and the issue of willingness to pay for heat resilient infrastructure in Chongqing, China, *Sustain. Cities and Society* 75 (2021) 103361.
- [53] I.A. Rana, L. Sikander, Z. Khalid, A. Nawaz, F.A. Najam, S.U. Khan, A. Aslam, A localised index-based approach to assess heatwave vulnerability and climate change adaptation strategies: a case study of formal and informal settlements of Lahore, Pakistan, *Environ. Impact Assess. Rev.* 96 (2022) 106820.
- [54] X.B. Zhang, J. Sun, Y. Fei, C. Wei, Cooler rooms on a hotter planet? Household coping strategies, climate change, and air conditioning usage in rural China, *Energy Res. Social Sci.* 68 (2020) 101605.
- [55] J. Kim, H. Kwon, Calculation of a climate change vulnerability index for nakkdong watersheds considering non-point pollution sources, *Appl. Sci.* 12 (9) (2022) 4775.
- [56] F. Cao, Y. Ge, J.F. Wang, Optimal discretization for geographical detectors-based risk assessment, *Geosci Remote Sens* 50 (1) (2013) 78–92.
- [57] J.F. Wang, C.D. Xu, GeoDetector: principle and prospective, *Acta Geogr. Sin.* 72 (1) (2017) 116–134.
- [58] J. Wang, M. Hu, F. Zhang, B. Gao, Influential factors detection for surface water quality with geographical detectors in China, *Stochastic Environ. Res. Risk Assessm.* 32 (2018) 2633–2645.
- [59] H. Wang, F. Qin, C. Xu, B. Li, L. Guo, Z. Wang, Evaluating the suitability of urban development land with a GeoDetector, *Ecol. Indic.* 123 (2021) 107339.
- [60] X. Wang, Y. Sun, L. Zhang, Y. Mei, Spatial variation and influence factor analysis of soil heavy metal as based on GeoDetector, *Stochastic Environ. Res. Risk Assessm.* (2021) 1–10.
- [61] S. Huang, L. Xiao, Y. Zhang, L. Wang, L. Tang, Interactive effects of natural and anthropogenic factors on heterogenic accumulations of heavy metals in surface soils through GeoDetector analysis, *Sci. Total Environ.* 789 (2021) 147937.
- [62] Y. Zhang, Y. Hu, D. Zhuang, A highly integrated, expandable, and comprehensive analytical framework for urban ecological land: a case study in Guangzhou, China, *J. Clean. Prod.* 268 (2020) 122360.
- [63] M. Jowkar, H.B. Rijal, J. Brusey, A. Montazami, S. Carlucci, T.C. Lansdown, Comfort temperature and preferred adaptive behaviour in various classroom types in the UK higher learning environments, *Energy Build.* 211 (2020) 109814.
- [64] S.J. Lloyd, M. Quijal-Zamorano, H. Achebak, S. Hajat, R. Muttarak, E. Striessnig, J. Ballester, The direct and indirect influences of interrelated regional-level sociodemographic factors on heat-attributable mortality in Europe: insights for adaptation strategies, *Environ. Health Perspect.* 131 (8) (2023) 087013.
- [65] P.D. Howe, J.R. Marlon, X. Wang, A. Leiserowitz, Public perceptions of the health risks of extreme heat across US states, counties, and neighborhoods, *Proc. Natl Acad. Sci.* 116 (14) (2019) 6743–6748.
- [66] A. Eady, B. Dreyer, B. Hey, M. Riemer, A. Wilson, Reducing the risks of extreme heat for seniors: communicating risks and building resilience, *Health Promot. Chronic Dis. Prev. Canada: Res., Policy, and Practice* 40 (7–8) (2020) 215.
- [67] ... & E.A.S. Mayrhuber, M.L. Dückers, P. Wallner, A. Arnberger, B. Allex, L. Wiesböck, R. Kutalek, Vulnerability to heatwaves and implications for public health interventions—A scoping review, *Environ. Res.* 166 (2018) 42–54.

- [68] K.R. Gunawardena, M.J. Wells, T. Kershaw, Utilising green and blue space to mitigate urban heat island intensity, *Sci. Total Environ.* 584 (2017) 1040–1055.
- [69] A. Onishi, X. Cao, T. Ito, F. Shi, H. Imura, Evaluating the potential for urban heat-island mitigation by greening parking lots, *Urban Forestry & Urban Greening* 9 (4) (2010) 323–332.
- [70] L. Nesbitt, D.L. Sax, J. Quinton, L.M. Harris, C.O. Barona, C. Konijnendijk, Greening practitioners worry about green gentrification, but many don't address it in their work, *Ecol. Soc.* 28 (4) (2023).
- [71] ... & C.Y. Wright, A. Mathee, C. Goldstone, N. Naidoo, T. Kapwata, B. Wernecke, D. A. Millar, Developing a healthy environment assessment tool (HEAT) to address heat-health vulnerability in South African towns in a warming world, *Int. J. Environ. Res. Public Health* 20 (4) (2023) 2852.
- [72] ... & M. Dinu Roman Szabo, A. Dumitras, D.M. Mircea, D. Doroftei, P. Sestras, M. Boscaiu, A.F. Sestras, Touch, feel, heal. The use of hospital green spaces and landscape as sensory-therapeutic gardens: a case study in a university clinic, *Front Psychol* 14 (2023) 1201030.
- [73] R.D. Meade, A.P. Akerman, S.R. Notley, R. McGinn, P. Poirier, P. Gosselin, G. P. Kenny, Physiological factors characterizing heat-vulnerable older adults: a narrative review, *Environ. Int.* 144 (2020) 105909.
- [74] C. Fastl, A. Arnberger, V. Gallistl, V.K. Stein, T.E. Dorner, Heat vulnerability: health impacts of heat on older people in urban and rural areas in Europe, *Wien. Klin. Wochenschr.* (2024) 1–8.
- [75] J. Van Hoof, H.R. Marston, J.K. Kazak, T. Buffel, Ten questions concerning age-friendly cities and communities and the built environment, *Build. Environ.* 199 (2021) 107922.
- [76] I. Grigorescu, I. Mocanu, B. Mitrică, M. Dumitrașcu, C. Dumitrică, C.S. Dragotă, Socio-economic and environmental vulnerability to heat-related phenomena in Bucharest metropolitan area, *Environ. Res.* 192 (2021) 110268.
- [77] K. Lanza, J. Jones, F. Acuña, M. Coudert, R.P. Bixler, H. Kamath, D. Niyogi, Heat vulnerability of Latino and Black residents in a low-income community and their recommended adaptation strategies: a qualitative study, *Urban Climate* 51 (2023) 101656.
- [78] G. Owen, What makes climate change adaptation effective? A systematic review of the literature, *Glob. Environ. Chang.* 62 (2020) 102071.
- [79] Z. Cai, Y. Tang, K. Chen, G. Han, Assessing the heat vulnerability of different local climate zones in the old areas of a Chinese megacity, *Sustainability* (2019), <https://doi.org/10.3390/SU11072032>.
- [80] W. Zhang, C. Zheng, F. Chen, Mapping heat-related health risks of elderly citizens in mountainous area: a case study of Chongqing, *Sci. Total Environ.* 663 (2019) 852–866, <https://doi.org/10.1016/j.scitotenv.2019.01.240>.
- [81] Z. Xiang, H. Qin, B.J. He, G. Han, M. Chen, Heat vulnerability caused by physical and social conditions in a mountainous megacity of Chongqing, *Sustainable Cities and Society* 80 (2022) 103792.
- [82] Cirendunzhu L. Bai, A. Woodward, Q. Liu, County-level heat vulnerability of urban and rural residents in Tibet, *Environ. Health* 15 (2016) 1–10.
- [83] ... & Z. Li, J. Hu, R. Meng, G. He, X. Xu, T. Liu, W. Ma, The association of compound hot extreme with mortality risk and vulnerability assessment at fine-spatial scale, *Environ. Res.* 198 (2021) 111213.
- [84] Y. Yin, A. Grundstein, D.R. Mishra, L. Ramaswamy, N.H. Tonekaboni, J. Dowd, DTE_x: a dynamic urban thermal exposure index based on human mobility patterns, *Environ. Int.* 155 (2021) 106573.
- [85] S.E. Kershaw, A.A. Millward, A spatio-temporal index for heat vulnerability assessment, *Environ. Monit. Assess.* 184 (2012) 7329–7342.
- [86] L. Barron, D. Ruggieri, C. Branas, Assessing vulnerability to heat: a geospatial analysis for the City of Philadelphia, *Urban Science* 2 (2) (2018) 38, <https://doi.org/10.3390/urbansci2020038>.
- [87] X. Wu, Q. Liu, C. Huang, H. Li, Mapping heat-health vulnerability based on remote sensing: a case study in Karachi, *Remote Sens (Basel)* 14 (7) (2022) 1590.
- [88] W. Zhang, C. Zheng, F. Chen, Mapping heat-related health risks of elderly citizens in mountainous area: a case study of Chongqing, *Sci. Total Environ.* 663 (2019) 852–866.
- [89] G. Falchetta, E. De Cian, I. Sue Wing, D. Carr, Global projections of heat exposure of older adults, *Nat. Commun.* 15 (1) (2024) 3678.
- [90] Y.H. Lim, M.L. Bell, H. Kan, Y. Honda, Y.L.L. Guo, H. Kim, Economic status and temperature-related mortality in Asia, *Int. J. Biometeorol.* 59 (2015) 1405–1412.